

**SEDIMENTOLOGY AND PETROLEUM POTENTIAL  
ASSESSMENT OF A SECTION OF THE EOCENE BENDE-  
AMEKI FORMATION, ANAMBRA BASIN, NIGERIA**

By

**Rotifa Samuel Oladeji**

**GLY/14/2264**

**A PROJECT WORK SUBMITTED TO THE DEPARTMENT  
OF GEOLOGY, FACULTY OF SCIENCE, FEDERAL  
UNIVERSITY OYE-EKITI**

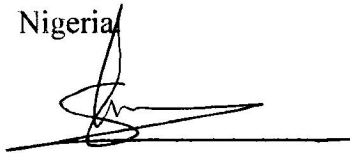
IN

**Partial Fulfillment of the Requirements for the Award of  
Bachelor of Science (B.Sc.) Degree in Geology**

**February, 2019.**

## CERTIFICATION

This is to certify that the research project on the Sedimentology and Petroleum Potential Assessment of a Section of the Eocene Bende-Ameki Formation, Anambra Basin, Nigeria was actually carried out by Rotifa Samuel Oladeji with matriculation number GLY/14/2264 under the supervision of Mr. M. O. Adeoye. The work has been approved as meeting the required standard for the award of Bachelor of Science (B.Sc.) Degree of the department of Geology, Faculty of Science, Federal University Oye-Ekiti, Ekiti State, Nigeria



.....  
Mr. Adeoye M.O.  
Project Supervisor

18/02/2019  
.....

Date

.....  
Prof. O.J. Ojo  
Head of Department

.....

Date

Prof. S.A. Opeyeye  
.....  
External Examiner

.....  
Date

## DEDICATION

I dedicate this report to Almighty God, to my parents Evangelist and Mrs. Rotifa to my friends and all my course mates.

## ACKNOWLEDGEMENTS

First of all I will like to thank the Lord Most High for His grace and Mercy throughout this project work.

A big thank you to my parents Evangelist and Mrs. Rotifa for their prayers, support and for their undying financial assistance to ensure success of my project work.

An undying appreciation goes to my Head of Department Professor O. J. Ojo and all the lecturers of the department of Geology for their contribution to my academic development.

A reserved appreciation goes to my supervisor Mr. Adeoye for his advice, time, attention and patience to ensure the completion of my B.Sc. project.

A big appreciation goes to my friends and course mates for their support and intellectual contribution during the course of the project work.

## TABLE OF CONTENTS

Title	i
Certification	ii
Dedication	iii
Acknowledgements	iv
Table of contents	v
List of Figures	viii
List of Tables	x
Abstract	xi
<b>Chapter One: Introduction</b>	<b>1</b>
1.1 General statement	1
1.2 Location of the study area	1
1.3 Geomorphology and Climate	1
1.4 Objectives of study	2
<b>Chapter Two: Geological Setting</b>	<b>4</b>
2.1 General statement	4
2.2 Evolution of the Benue Trough	4
2.3 Anambra Basin	5
2.3.1 The Nkporo Group	5
2.3.2 The Mamu Formation	8
2.3.3 The Ajali Formation	8
2.3.4 The Nsukka Formation	8
2.3.5 The Imo Formation	10

2.3.6 The Ameki Group	10
2.3.7 The Ogwashi-Asaba Formation	10
<b>Chapter Three: Methodology</b>	<b>12</b>
3.1 General statement	12
3.2 Materials	12
3.2.1 Field Mapping	12
3.2.1.1 Logging	13
3.2.1.2 Sampling Collection	13
3.3 Laboratory Analysis	13
3.3.1 Granulometric analysis	13
3.3.2 Petrography	14
3.3.3 Rock-Eval Pyrolysis	15
<b>Chapter Four: Result and Discussion</b>	<b>16</b>
4.1 Lithofacies Description	16
4.1.1 Claystone-siltstone facies	16
4.1.2 Sandstone facies	16
4.1.3 Shale facies	18
4.1.4 Ironstone facies	18
<b>4.2 Sedimentary Structure</b>	<b>22</b>
<b>4.2.1 Planar cross stratification</b>	<b>22</b>
<b>4.2.2 Herringbone cross stratification</b>	<b>22</b>
<b>4.3 Grain size analysis</b>	<b>24</b>
<b>4.4 Petrography</b>	<b>32</b>

<b>4.1 Mineralogy</b>	32
<b>4.2 Classification of the sandstone</b>	37
<b>4.5 Organic Geochemistry</b>	39
<b>4.5.1 Total Organic Carbon</b>	39
<b>4.5.2 Hydrogen index (HI)</b>	39
<b>4.5.3 Thermal Maturity</b>	40
<b>4.5.4 Generative Potential</b>	40
<b>4.5.5 Kerogen Type</b>	40
<b>Chapter Five: Conclusions</b>	<b>45</b>
5.1 Conclusions	45
References	46
Appendix	51

## LIST OF FIGURES

Figure	Title	Page
1.1	Geological map of Nigeria showing Anambra Basin	3
2.1	The tectonic evolution of the Benue Trough	6
2.2	Map of Nigeria showing the Benue Trough	7
2.3	Geological map of south eastern Nigeria showing formations of the Anambra Basin	9
2.4	Stratigraphy of the Southern Benue Trough and the Anambra Basin	11
4.1	Lithologic section of the Bende-Ameki Formation	17
4.2	Claystone with embedded carbonaceous shale at the top of the section	19
4.3	Clayey siltstone overlying laminated shale	19
4.4	Ferruginized silty claystone of the Bende-Ameki Formation	20
4.5	Grey shale with embedded nodules	20
4.6	A medium bedded ironstone of the Bende-Ameki Formation.	21
4.7	Planar cross stratified medium grained sandstone showing an inclined unidirectional structure	23
4.8	Ferruginized herringbone cross stratified medium grained sandstone showing an inclined unidirectional structure	23
4.9	Graph of grain size distribution for sample OS10.	25
4.10	Graph of grain size distribution for sample OS11.	26
4.11	Graph of grain size distribution for sample OS12.	27
4.12	Graph of grain size distribution for sample OS13.	28
4.13	Graph of grain size distribution for sample OS14.	29
4.14	Scatter plot of (A) skewness against standard deviation, (B) mean against standard deviation .	31
4.15	Photomicrograph of sandstone sample OS 13 showing the mineralogical composition and texture under cross polar	34
4.16	Photomicrograph of sandstone sample OS 06 showing the mineralogical composition and texture under cross polar	35
4.17	Photomicrograph of sandstone sample OS 14 showing the mineralogical composition and texture under cross polar	36
4.18	Ternary plots for the classification of sandstones of the Bende-Ameki formation	38



4.19	Graph of HydrogenIndex(HI) against Tmax.	41
4.20	Graph of Hydrogen Index (HI) against Oxygen Index (OI).	42
4.21	Graph of S2 against TOC.	43
4.22	Graph of PI against Tmax.	44

## LIST OF TABLES

Table	Title	Page
4.1	Table of grain size data for sample OS10	25
4.2	Table of grain size data for sample OS11	26
4.3	Table of grain size data for sample OS12	27
4.4	Table of grain size data for sample OS13	28
4.5	Table of grain size data for sample OS14	29
4.6	Grain size analysis interpretation.	30
4.7	Quantitative mineralogical composition of sandstones of the Bende-Ameki Formation.	33
4.8	Relative abundance of sandstone framework components.	37
4.9	Rock-Eval data of the shale samples	49

## ABSTRACT

The Eocene Bende-Ameki Formation constitute one of the Formations of the Anambra Basin. Exposed rocks in this formation consist of shale, claystone, siltstone, sandstone, and ironstone facies. This study has investigated the sedimentology and petroleum potential assessment of a section of the Formation exposed along Onitsha-Awka express roads through granulometric, petrographic and organic geochemical analysis respectively.

Granulometric result shows that the sandstones of the study area have an average mean, skewness, standard deviation and kurtosis of  $1.36\Phi$ ,  $-0.038\Phi$ ,  $0.82\Phi$  and  $1.32\Phi$  respectively. This indicates that the sandstone samples are medium grained, near symmetrical, moderately sorted and leptokurtic. These indications are typical of fluvial environment. The environment of deposition was further confirmed by scatter plots of skewness against standard deviation, and mean against standard deviation to be fluvial.

Petrographic result used to estimate the QFR modal composition of the sandstones reveals the predominance of quartz ranging from 66-88% (average of 76.2%), with feldspars ranging from 10-24% (average of 16%) and rock fragments ranging from 2-15% (average of 8%). The ternary diagram plotted indicates that the sandstone samples are subarkose and lithic subarkose.

The Total Organic Carbon (TOC) of the shales range from 0.46 to 5.08wt% (mean of 2.56wt) suggesting that they have good level of organic matter that can generate hydrocarbon. This was confirmed by the petroleum source potential (S1 +S2) that range from 0.46 to 9.03mgHc/g TOC (mean of 3.45mgHc/g TOC). The HI values range from 79 to 158mgHC/gTOC (mean of 103.8mgHC/gTOC), indicating a Type III gas prone kerogen for the shales. Also, the thermal maturity values of the shales range from 424 to 431°C revealing that they are immature to marginally matured.

## CHAPTER ONE

### INTRODUCTION

#### 1.1 General Statement

A study was carried out on a section of the Bende-Ameki Formation of the Cretaceous – Tertiary Anambra Basin to evaluate the depositional condition of the clastic sediments and the petroleum potential of the organic sediments. The lithologic section of the Bende-Ameki Formation studied was exposed along the Onitsha-Awka express road. The formation is underlain by the Paleocene Imo shale and overlain by the Oligocene Ogwashi Asaba Formation. The age of the Formation has been considered to be Early – Middle Eocene (Bergren, 1960; Adegoke, 1969; Arua, 1986).

#### 1.2 Location of the Study Area

The study area for this project lies within the southern Anambra Basin (Fig.1.1), and it is covered by lithologic successions of the Bende - Ameki formation. The outcrop is exposed along the Onitsha-Awka express road between Latitude  $06^{\circ}10' 51.5''$  -  $06^{\circ}10' 50.7''$  and Longitude  $006^{\circ}51' 54.1''$  -  $006^{\circ}51' 51.6''$ . It consists predominantly of rhythmic clastic sequences of sandstones, siltstones, ironstone bands, claystones with interbedded shales.

#### 1.3 Geomorphology and Climate

As in most of West Africa, Nigeria's climate is characterized by strong latitudinal zones becoming progressively drier from the coastal region to the north. Rainfall is the key climatic variable, and there is a marked alteration of wet and dry seasons. The rainy season starts from March to October while the dry season starts in November and ends in February the following year. The Benue Trough falls within the equatorial climatic region of West Africa. The mean annual temperature ranges from  $19^{\circ}\text{C}$  to  $31^{\circ}\text{C}$ . The study area form part of the Guinea Savannah region of Nigeria and typical trees found includes: mahogany, oak, locust, shear-butter and palm trees forming scattered patches of woodland with tall grasses. The elevation pattern of most of the study area consists of gradual rise from the coastal plains to the northern savannah regions, generally reaching an elevation of 600 to 700 meters. Lignite occur in a generally undulating, deeply incised and low to moderate altitudes ranging from less than 50m to almost 160m in the northern most part of the study area. The climate is classified as tropical, the rainfall here averages 1828 mm. Precipitation is the lowest in December, with an average of 12 mm. In September, the precipitation reaches its peak, with

an average of 316 mm, with about four months of dryness (November to February). The average annual temperature in the study area is 27.0°C, at an average temperature of 28.9 °C, March is the hottest month of the year, at 25.4 °C on average, July is the coldest month of the year.

#### **1.4 Objectives of Study**

The principal purposes for this study include:

- i. To deduce the environment of deposition of the siliciclastic sediments.
- ii. To ascertain the mineralogical constituents of the sandstones.
- iii. To provide information on the Kerogen types present in the source rock and likewise evaluate the petroleum potential.

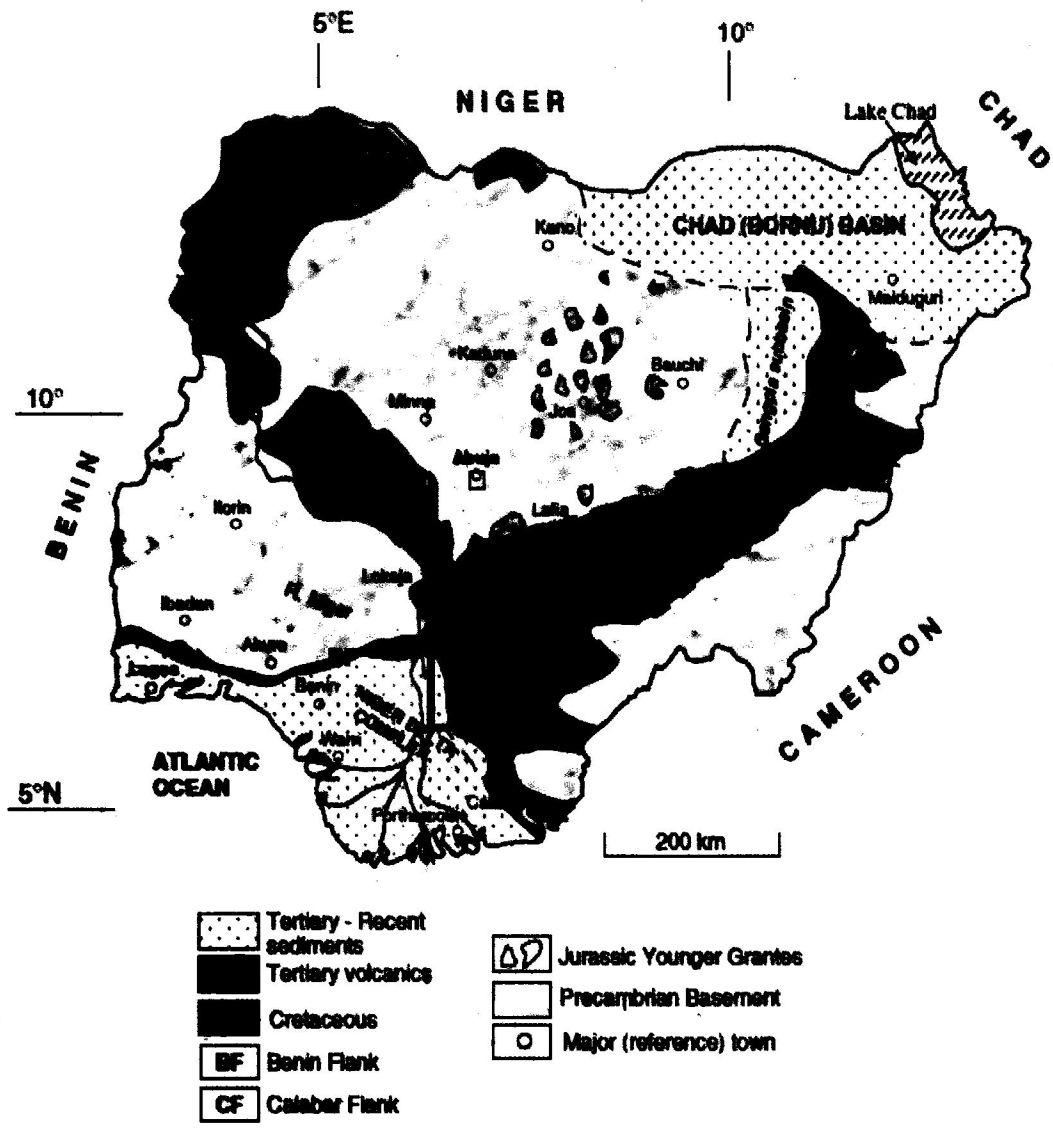


Fig. 1.1: Geological map of Nigeria showing Anambra Basin (modified from Obaje, 2009)

## CHAPTER TWO

### GEOLOGICAL SETTING

#### 2.1 General Statement

Sedimentary Basins in Nigeria are related to the tectonic processes of the break-up of the Gondwanaland. The basins which are formed either by the spreading edge of the continent or the tension generated by the divergent tectonics, are believed to be relics of the fragmentations which led to the separation of the African and South-American plates as well as the formation of the South Atlantic ocean. The opening of the Atlantic in the early Mesozoic era triggered the crustal fragmentation of West- Central African Craton into a rift system. The basins are all rift related and consist of sediment fill which differently are between Cretaceous to Tertiary. The geologic basins of Nigeria include; Dahomey, Bida, Sokoto, Chad, Anambra, Benue Trough and Niger Delta. The study area falls under the Anambra Basin which is a sub-basin under the Lower division of the Benue Trough.

#### 2.2 Evolution of the Benue Trough

The tectonic history of Benue Trough, South-eastern Nigeria dates back to the Pre- Albian times. According to Burke et.al (1972), Nwachukwu (1972), the Abakaliki-Benue Trough originated as a failed arm of the triple junction rift-ridge system, which led to the separation of Africa from South America during the Aptian/Albian (Fig. 2.1). The opening of these arms started in Mid Aptian in the Southern Atlantic by crustal stretching and downwarping, accompanied by the development of coastal evaporites basins. It reached the Gulf of Guinea by Late Albian and extended North East, to form the Benue Trough. However the Northeast-South West (NE-SW) trending Benue Trough is thought to be the result of the Pre-Albian rifting of the African Shield, prior to the opening of the south Atlantic (Uzuakpunwa, 1974).

Murat (1970) identified three main tectonic phases in the Benue Trough which controlled the basin filling. The first phase began during Albian and was characterized by movements along major NE-SW trending Benue–Abakaliki Trough. This led to the emergence of two stable areas on either side of the Benue–Abakaliki Trough, called the Anambra platform on the west and Ikpe Platform on the East. The NW-SE trending Ikang Trough, Ituk High and the Eket Platform are found on the eastern flank, and all persisted into the Tertiary without Significant changes.

A second major tectonic event (compressional movements along the established NE-SW trend), caused a generalized folding which affected the Cretaceous sediments in the Benue Trough (Benkhelil, 1986). This led to a series of NE-SW trending folds that resulted in the Abakaliki Anticlinorium, and the subsequent downwarping of the Anambra Platform, to form the wide Anambra basin (Fig. 2.2) and the narrow Afikpo Synclinorium on the west and east of the Abakaliki Anticlinorium respectively (Kogbe, 1976). The depressions became the main depositional targets from Campanian to Paleocene. The onset of this folding phase in the Late Santonian was accompanied by pronounced igneous activities. These account for the occurrence of massive deposits of intermediate and basic intrusive rocks found at Abakaliki, Ishiagu, Lokpaukwu, Akpoha and some other localities within the region.

The intensity of the folding varies greatly from NE to SW and locally from the axis towards the edges of the basin. The effects of the Santonian tectonic phase are restricted to the Abakaliki Anticlinorium in the Southern Benue Trough. This second tectonic phase was interpreted as the closing of an embryo Benue Ocean (Burke et.al, 1971), and was as a result of differential movement between two parts of the African plate as a consequence of differences in the rate of spreading and direction between the section of the Mid Atlantic Ridge opposite the bulge of Africa and also south of the Gulf of Guinea. The exposures of the Coniacian, Turonian and Albian Formations were eroded as a result of the uplift and folding of the Abakaliki Anticlinorium.

### **2.3 The Anambra Basin**

The second tectonic phase resulted to the Santonian folding and upliftment of the Abakaliki region and the accompanying shift of the depocenter into the Anambra Basin and the Afikpo Syncline. This episode saw to the deposition of the Nkporo Group, Mamu, Ajalli, Nsukka, Imo Formations, Ameki Group and Ogwashi-Asaba Formation (Fig. 2.3 and Fig. 2.4).

#### **2.3.1 The Nkporo Group**

The Nkporo Group is made up of three members— Afikpo/Owelli Sandstone, Nkporo and Enugu Shales. The arenaceous facies of the Afikpo and Owelli Sandstones are lateral equivalents to the Nkporo Formation in the Afikpo and Anambra Basins respectively. According to Odumoso et.al (2013), the Owelli Sandstone is an elongate shoestring sand body to the northwest defining a meander belt of fluvial channel system and a fluvial point bar. It is massively bedded, hard and often ferruginous (in some parts) and friable.



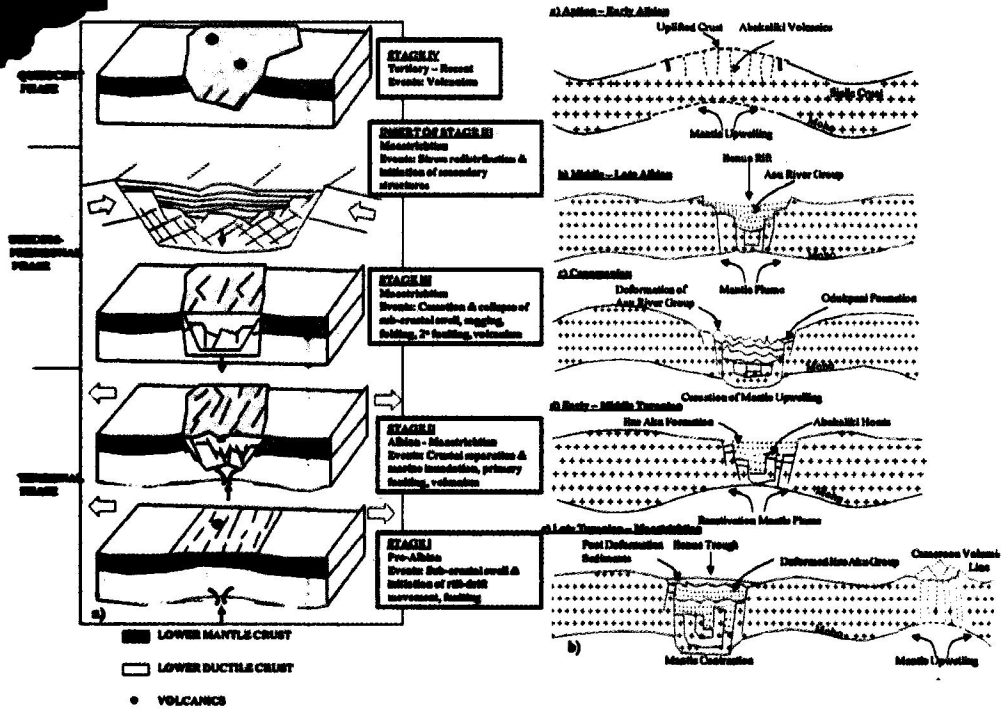


**Fig. 2.1: Models for the RRR Rift origin of the Benue Trough of Nigeria. (a) Spreading Ridge Model (Avbovbo et. al, 1986); (b) Aulacogen Model (from Olade, 1975)**

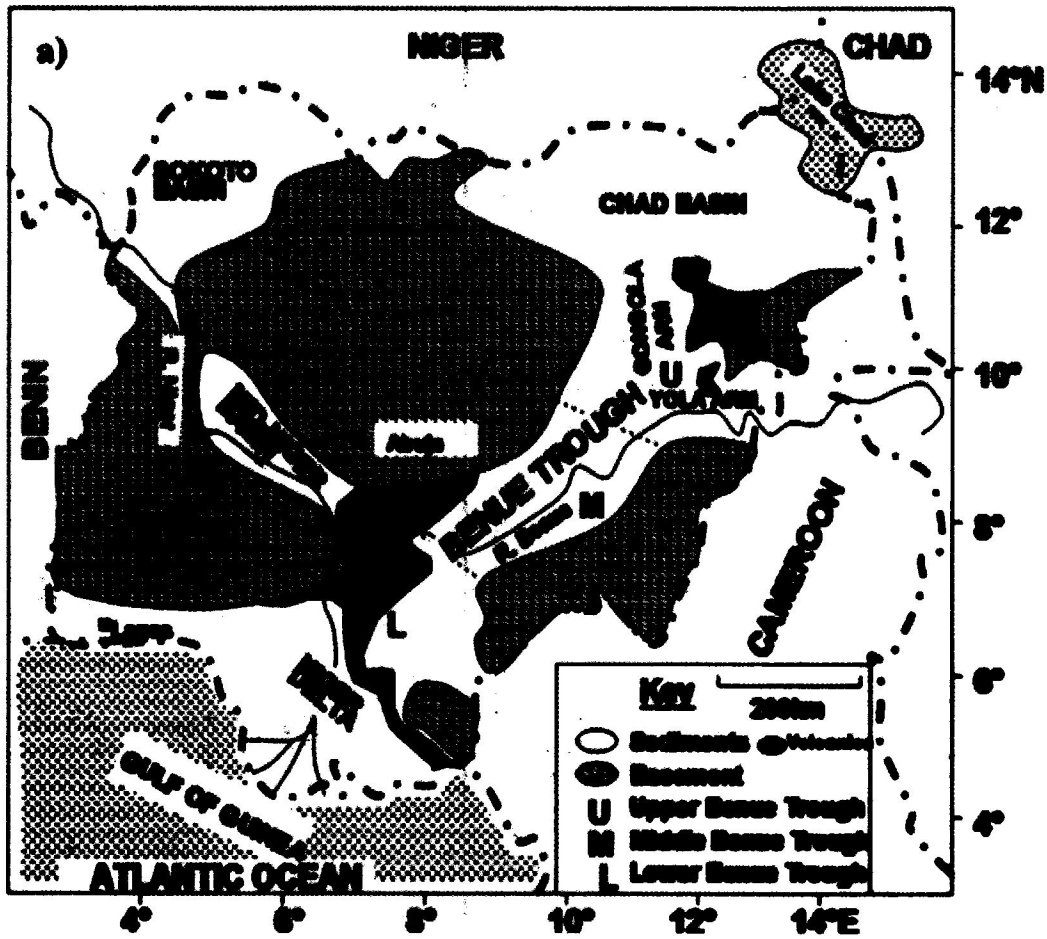


Fig. 2.2: Generalized geological map of Nigeria Showing the Benue Trough. Note that the blue area represents the Anambra Basin (Abubakar, 2014).

The Enugu Shales are made up of carbonaceous shales and coals with the upper half deposited in lower floodplain and swampy environments; overlie the Nkporo Formation (Ladipo et.al, 1992). The sediments have a poorly developed foreshore and shore face with extensive coastal swamps and were assigned Campanian to Lower Maastrichtian based on diagenetic species of palynomorphs such as *Cingulatisporitesornatus* and *Tricolpitesieniabaensis* (Reyment and Morner, 1977).

### **2.3.2 The Mamu Formation**

The deposits of the transgressive Nkporo cycle was overlain by the Lower Maastrichtian sandstones, shales, siltstones and mudstones and the interbedded coal seams of the deltaic Mamu Formation in most parts of the Anambra Basin (Akande et.al, 2010). It is known as the Lower Coal Measures, and contains marine intercalations composed of ammoniferous shales (Reyment, 1964).

### **2.3.3 The Ajali Formation**

The Ajali Formation overlies the Mamu Formation (Obi, 2000). It is mainly unconsolidated, poorly sorted, coarse-fine grained sandstone, poorly cemented; mudstone and siltstone, and is dated Mid to Late Maastrichtian. The sandstone is typically white in colour but in some cases, iron-stained. Thin bands of white mudstone and shale in the Ajali Formation occur at intervals and increases in number towards the base.

### **2.3.4 The Nsukka Formation**

The diachronous Nsukka Formation (Late Maastrichtian - Early Paleocene) which is also known as the "Upper Coal Measures" conformably overlies the Ajalli Sandstone (Reyment, 1965) (Obi, 2000). It is comprised mainly of interbedded shales, siltstones, sands and thin coal seams, which have become laterized in many places where they characteristically form resistant capping on mesas and buttes (Uzoegbu et.al, 2013). The basal bed begins with coarse to medium-grained sandstones and passes upward into well-bedded blue clays, fine-grained sandstones, and carbonaceous shales with thin bands of limestones (Reyment, 1965) (Obi et.al, 2001). The Nsukka Formation as well as the overlying Imo Shale marked the onset of another transgression in the Anambra Basin during the Paleocene.

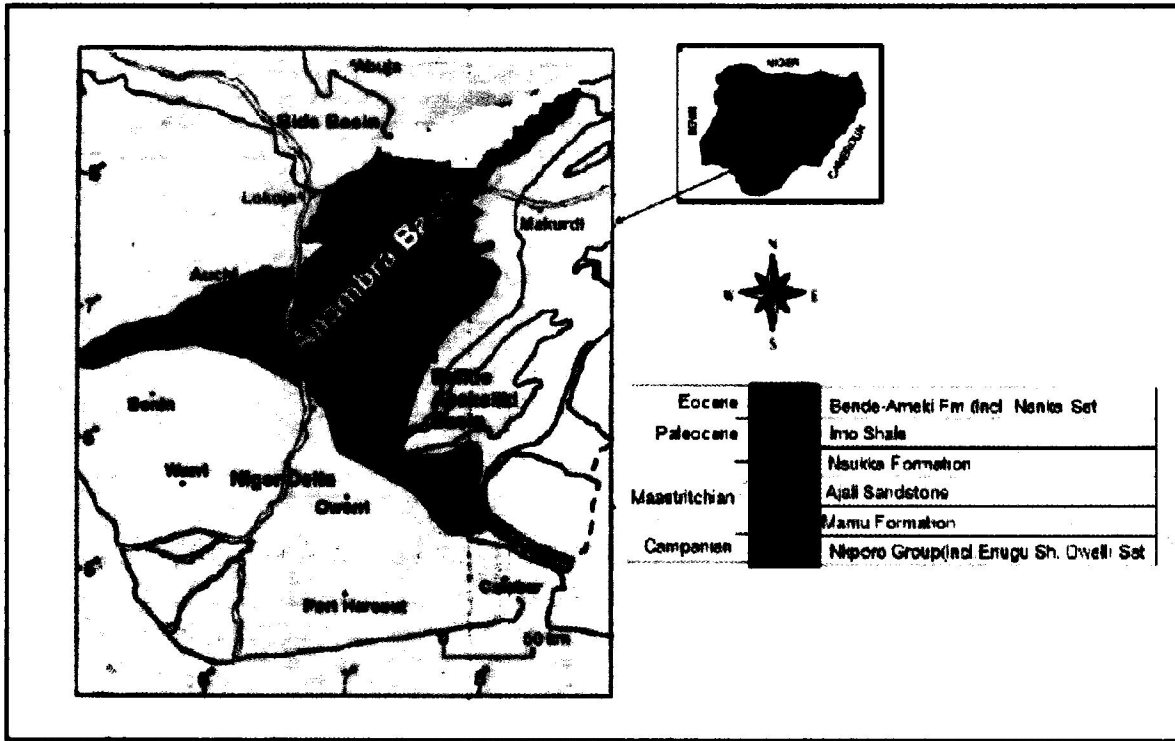


**Fig. 2.3:** Geological map of south eastern Nigeria showing formations of the Anambra Basin (Salufu and Ogunkunle, 2015)

### **2.3.5 The Imo Formation**

The Imo Formation consists of blue-grey clay, sand, shales, and black shales with bands of calcareous sandstone, marl, and limestone (Reyment, 1965), with a maximum thickness of about 500 meters. It marks the onset of another transgression in the Anambra Basin during the Paleocene. This Paleocene transgression also deposited its lateral equivalents - the Ewekoro Formation in south western Nigeria. The formation lies conformably on the Maastrichtian Nsukka Formation. The Imo Formation is said to be of Paleocene age as indicated by its ostracode and foraminifera biostratigraphy (Reyment, 1965), and microfauna recovered from the basal limestone unit (Adegoke et.al, 1980) (Arua, 1980).

### **2.3.6 The Ameki Group**

This is the regressive sandstone succession that overly the Imo Formation. The Eocene witnessed regression due to the uplift and erosion of folded sediment as a result of the post Maastrichtian folding movement that affected different parts of the country. Regression continued throughout the Eocene (Reyment, 1965). In the Abakaliki/Anambra basin areas the Ameki Group is made up of the Ameki Formation, Nanka and Nsugbe Sandstone. The formation consists of a series of highly fossiliferous greyish-green sandy clay with calcareous concretions and white clayey sandstones (Kogbe, 1989).

### **2.3.7 The Ogwashi-Asaba Formation**

This represents the last sedimentary deposit within the Anambra Basin. It lies unconformably on the Ameki Group. The Ogwashi-Asaba Formation comprises of alternating coarse grained sandstone, lignite seams, and light coloured clays of continental origin (Adeoye et al. 2016a; Kogbe, 1976). The age of the formation was suggested by Adeoye et al. (2016b); Reyment, (1965); Akande et.al, (2011) Nwajide, (1990), to be of Oligocene-Miocene, although palynological study by Jan Du Che<sup>^</sup>Ne et.al (1979) yielded a Mid Eocene age for the basal part. The Ameki Group and the overlying Ogwashi-Asaba Formation in the Southern Benue Trough and Anambra Basin are correlative with the Agbada Formation in the Niger Delta.

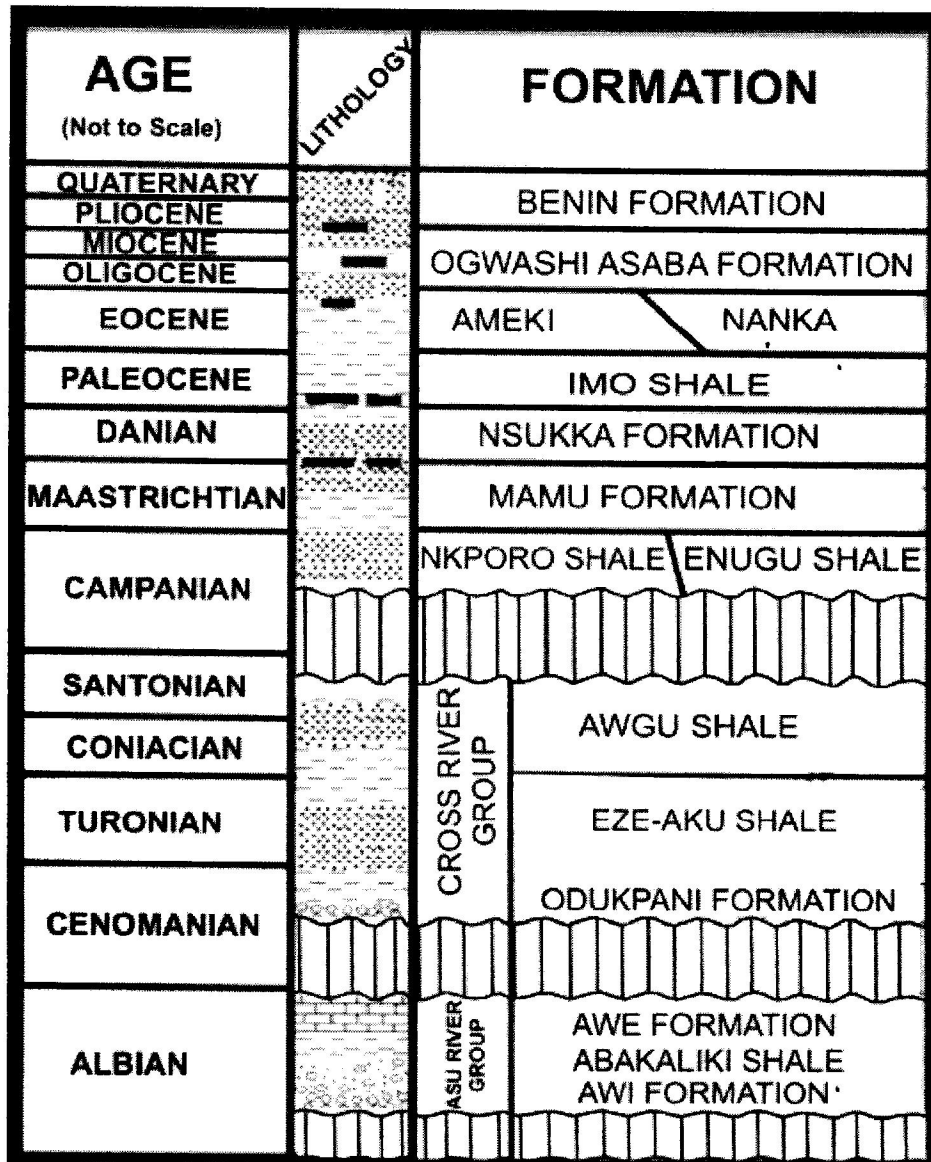


**Fig. 2.4:** Stratigraphy of the Southern Benue Trough and the Anambra Basin (modified from Akaegbobi et al., 2000).

## CHAPTER THREE

### METHODOLOGY

#### 3.1 General statement

This chapter includes methods applied in this research. These include; field mapping and laboratory analysis. The field mapping involves thorough logging at each location, sections measurement, descriptions, and collection of representative samples. Laboratory analysis were done on five (5) sandstone samples for grain size analysis, six (6) sandstone samples for petrography and five (5) shale samples for Rock Eval pyrolysis.

#### 3.2 Materials

**Measuring tape:** It is a ribbon of cloth which is well calibrated to measure the thickness of bed.

**Geological hammers:** It is a tool with a heavy head usually metal and a wooden handle used for hitting the chisel for sample collection.

**Chisel:** This is a cutting tool consisting of a slim metal which is sharp at one end and it is provided with a handle at the other end. It is used to collect fresh samples on field.

**GPS (Global Positioning System):** This is a device which enables the determination of precise location (longitude and latitude) and elevation based on signals received from the satellites while on field.

**Digital camera:** This is used in capture pictures of rock in-situ with the sedimentary structures.

##### 3.2.1 Field Mapping

The field work was done on the 26th January, 2018. The outcrop of the Bende-Ameki Formation mapped was a road exposure along the Onitsha-Awka express road which is between N06°10' 51.5" -06°10' 50.7" and E006°51' 54.1" - 006°51' 51.6". The field mapping involves thorough logging at each location, sections measurement, descriptions, and collection of representative samples. The field mapping exercise was carried out using

different equipment like GPS, hammer, chisel, measuring tapes, digital camera, marker, masking tapes, field notes and sample bags.

### **3.2.1.1 Logging**

Exposed stratigraphic section at Onitsha-Awka express road was logged accordingly and beds were identified based on grain size, texture, colour and sedimentary structures. The measurement of the thickness of each bed was done with the aid of a measuring tape from the basal bedding plain of the overlying bed to the top bedding plain of the underlying bed, and was represented on the field note.

### **3.2.1.2 Sample Collection**

Samples were taken with the aid of a geological hammer and chisel, carefully stored in a well labelled sample bag. Based on the field observations, textural, structural, and compositional characteristics of the outcrop, tentative names were given to rock samples taken from the outcrop.

## **3.3 Laboratory Analysis**

The laboratory study involved petrography (thin section), granulometric analysis, and Rock-Eval pyrolysis.

### **3.3.1 Granulometric Analysis**

The Standard grain size analysis test determines the relative proportions of different grain sizes as they are distributed among certain size ranges. Grain size distribution is one of the most important characteristics of sediment. Characterizing the physical properties of sediment is important in determining its suitability for various uses as well as studying sedimentary environments and geologic history. Instruments used include;

- i. Stack of Sieves including pan and cover
- ii. Weighing Balance
- iii. Mechanical sieve shaker

#### **Test Procedure;**

- i. Take the dried sandstone sample and weigh 100g.
- ii. If soil particles are lumped, crush the lump and not the particles using a pestle and a mortar.



- iii. Prepare a stack of sieves in a coarsening upward sequence. Sieves having larger mesh sizes (i.e. 4.00mm) are placed above the ones having smaller mesh sizes (i.e. 0.063mm). Particles less than 0.063mm are collected in the pan which is under the sieve with the smaller mesh size.
- iv. Make sure the sieves are clean, if there are grains stuck in the openings, it should be removed using a brush.
- v. Weigh all the empty sieves and the pan separately.
- vi. Pour the weighed sample and pour into the stack sieves (as arranged in step iii) from the top and place the cover, put the stack in the sieve shaker and fix the clamps, start the shaker and let it shake for about 10 to 15 minutes.
- vii. Stop the sieve shaker and measure the mass of each sieve + retained soil.
- viii. The data derived are then recorded in a table.

### 3.3.2 Petrography

Thin sections were prepared for six sandstone samples during the exercise in order to carry out the petrographic study. The sandstone samples were impregnated with resin. Impregnation of the samples was done using Canada balsam and Lakeside 70 cements in the same proportion and heated in a hot flame for a period of 30 minutes before thinning. The surface was smoothed with a Carborandum grits of different grades (90, 200, and 400). Glass slide were then labelled and the samples mounted on them using Araldite as adhesive, ensuring the mounts were bubble free. The samples were then heated on the electric drier and left to cool in free air.

The samples attached to the glass slide were then grinded down on the carborandum grit (i.e. mounted sample) from the coarse 400 to the finer 800 grade. Precautions were observed not to pluck the entire minerals away. The correct thicknesses were judged by examining the slide under microscope with cross polar. After the thicknesses were done, thin sections were thoroughly washed, and all remaining cement scraped away from around the chips. The glass slides were then covered with cover slip and pressed down to remove any air bubble. Excess cements were removed using methlylated spirits.

The prepared thin section were examined under a petrological microscope to identify the mineral assemblage, morphology and other properties while the minerals optical properties such as cleavage colour, relief etc. were studied under a Plane polarized Light (PPL) and

Cross polarized light (XPL) of the petrological microscope. The results attained from these analyses were subjected to interpretation to delineate the mineralogical, and modal composition of the rock types being analysed.

### 3.3.3 Rock-Eval Pyrolysis

Five shale samples were collected, washed, pulverized and analysed for Total Organic Carbon (TOC) by means of LECO – CS analyser. The hydrocarbon generation potential, maturity, type of Kerogen and Hydrogen Index (HI) values were determined using a Rock – Eval II instrument up to an elevated temperature of ca. 600°C (Akande et al. 2015). Pyrolysis of 30 – 40 mg of each sample at 300°C for 4 min was followed by programmed pyrolysis at 25°C/min to 550°C in an atmosphere of helium.

Rock-Eval pyrolysis provides evidence by direct estimation of the free already generated hydrocarbons in the rock (S1) and the hydrocarbons that can be generated from the Kerogen by thermal cracking (S2), S1+S2 represent the rocks total hydrocarbon generation potentials. Tissot and Welte, 1984 suggest that a hydrocarbon yield (S1+S2) less than 2 kgHC/t corresponds to little or no oil potential and some potential for gas, S1+S2 from 2 to 6 kgHC/t indicate moderate to fair source rock potential, and hydrocarbon yield above 6 kg HC/t indicate good to excellent source rock potential. The threshold of S1+S2 greater than 2 kgHC/t can be considered as prerequisite for classification as a possible oil source rock and provides the minimum oil content necessary for the main stage of hydrocarbon generation to saturate the pore network and permit expulsion.

Kerogen type could be identified from the HI values. Type I kerogen is hydrogen rich (HI greater than 600mg HC/g TOC) and this is considered to be predominantly oil prone. Type II Kerogen is characterized by HI between 350 and 600mg HC/g TOC and this can generate both oil and gas at appropriate level of maturity. Type III Kerogen is characterized by low to moderate HI of between 75 and 200mgHC/g TOC and could generate gas at the appropriate level of thermal maturity. However, humic coals (with Type III kerogen) may have HI up to 300mgHC/g TOC and possess the capacity to generate oil. Type IV Kerogen normally exhibits very low HI less than 50 mgHC/g TOC and is formed under oxic (wild fire) conditions.

## CHAPTER FOUR

### RESULT AND DISCUSSIONS

#### 4.1 Lithofacies Description

The section of the Bende-Ameki Formation exposed along the Onitsha-Awka express way consists of claystone-siltstone, sandstone, ironstone and shale facies (Fig. 4.1). The section is approximately 23m thick with 3.2m thick grey nodular shale at the base. This passes into a thin ironstone bed which is about 0.2m thick. Overlying it is 1.7m thick laminated shale which is likewise overlain by 1.2m thick clayey siltstone bed. Sitting on top of the siltstone is carbonaceous shale which is 1m thick. At the middle of the section, there are several varieties of medium grained sandstones with different sedimentary structure. These structures include planar cross bedding and herringbone cross stratification. Some of the sandstones are reworked and highly indurated, indicating the level of compaction. The sandstones varied in thickness from 0.4m to 1.6m. Overlying the sandstones is a thin bed of ironstone with 0.3m thick. The ironstone is subsequently overlain by 0.9m thick claystone with embedded shale. This passes into 2.7m thick fractured, laminated shale which is equally been underlain by 2m thick massive claystone. The section is been capped by 2m overburden.

##### 4.1.1 Claystone-Siltstone facies

This facies consists of claystones and siltstones. The siltstone bed is 1.2m thick and it consists of appreciable clay matrix (Fig. 4.2, Fig. 4.3 and Fig. 4.4). Four claystone beds were recorded with thickness ranging from 0.8m to 2.0m. The claystones are creamy and contain fractures. Siltstone and claystone facies are interpreted as floodplain deposit resulting from deposition out of suspension in an upper flow regime during flooding (Reading, 1981; Ojo and Akande, 2003).

##### 4.1.2 Sandstone facies

This facies consists of medium grained sandstone subfacies. The thicknesses range from 0.4 to 1.6m. At the middle of the section, the sandstone is highly indurated, indicating the level of compaction during the formation (Fig. 4.7 and Fig. 4.8). The medium grained sandstone facies are interpreted as braided fluvial deposits (Ojo and Akande, 2012).

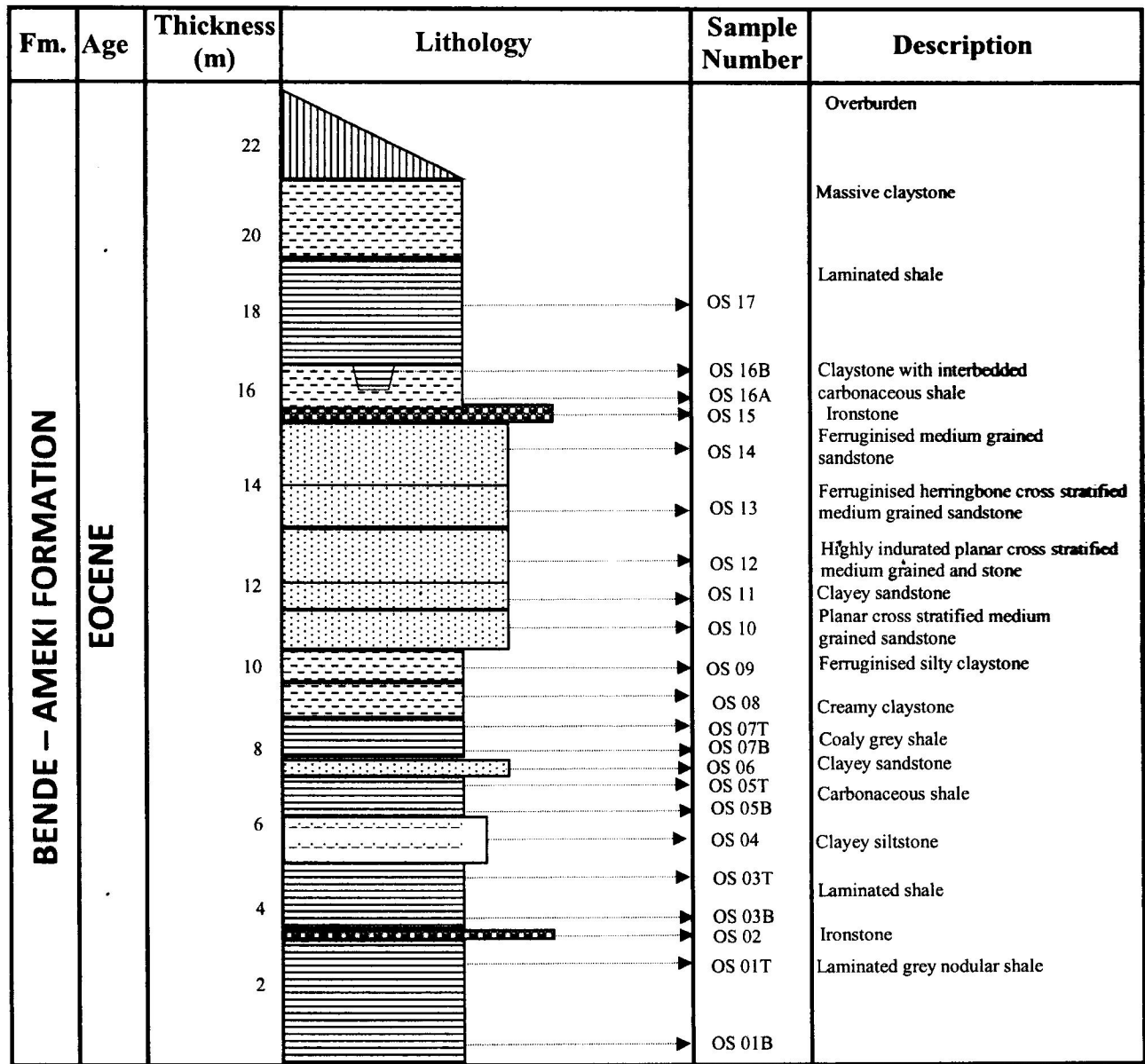


Fig. 4.1: Lithologic section of the Bende-Ameki Formation exposed along the Onitsha-Awka express road (Latitude - N06° 14' 50.7" and Longitude - E006° 51' 51.6").

### **4.1.3 Shale facies**

The shale facies observed in the section include; laminated, carbonaceous, coaly and nodular shale (Fig. 4.5). Their various thicknesses range from 1 to 3.2m. They are essentially grey to dark grey in colour indicating large content of organic matter. Lamination in the shale beds must have occurred as a result of sand infiltration during the time of deposition.

### **4.1.4 Ironstone facies**

Two ironstone beds were identified in the study area OS02 and OS15 with thicknesses of 0.2m and 0.3m respectively (Fig. 4.6). The ironstones are yellowish brown in colour. Ironstones are sedimentary rock that contains more than 15% iron, which may occur as goethite, siderite or hematite.



**Fig 4.2:** Claystone with embedded carbonaceous shale at the top of the section

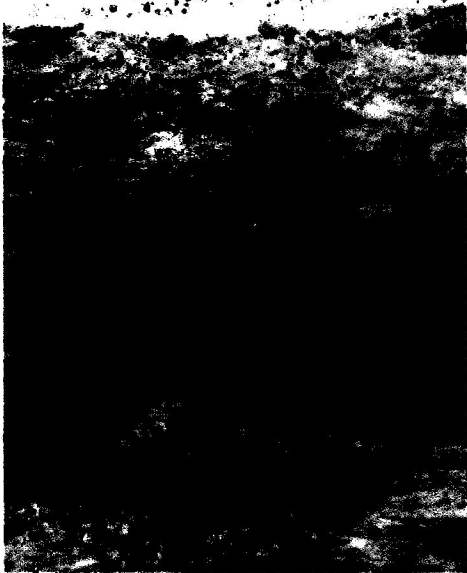


**Fig. 4.3:** Clayey siltstone overlying laminated shale. Notice the sharp sedimentary boundary between the beds

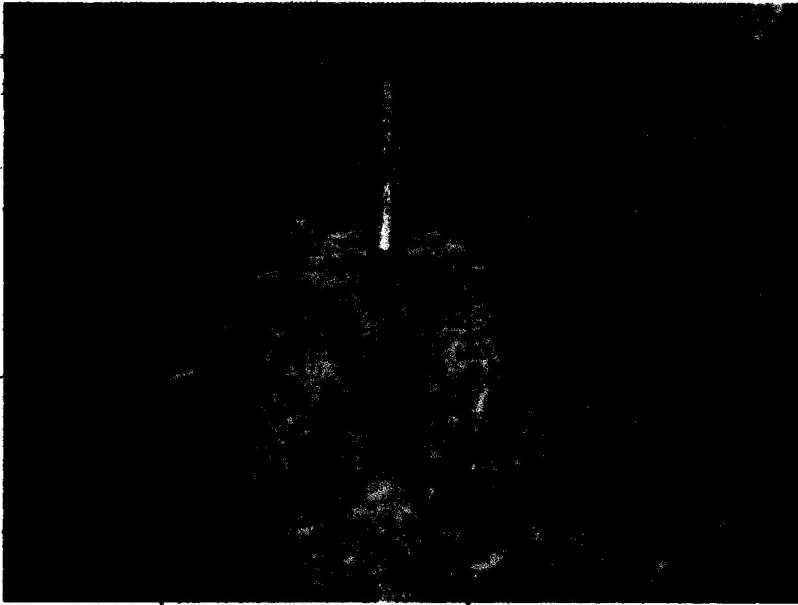


**Fig. 4.4:** Ferruginized silty claystone of the Bende-Ameki Formation

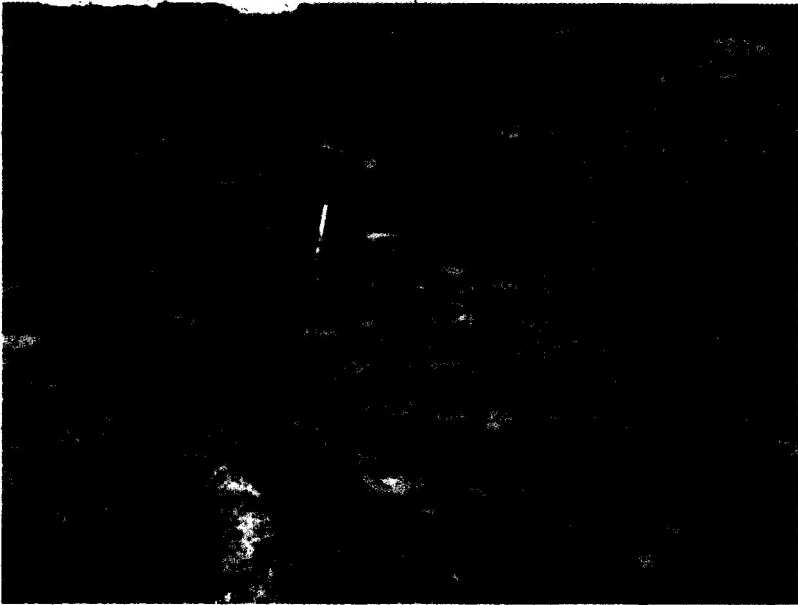


**Fig 4.5:** Grey shale with embedded nodules

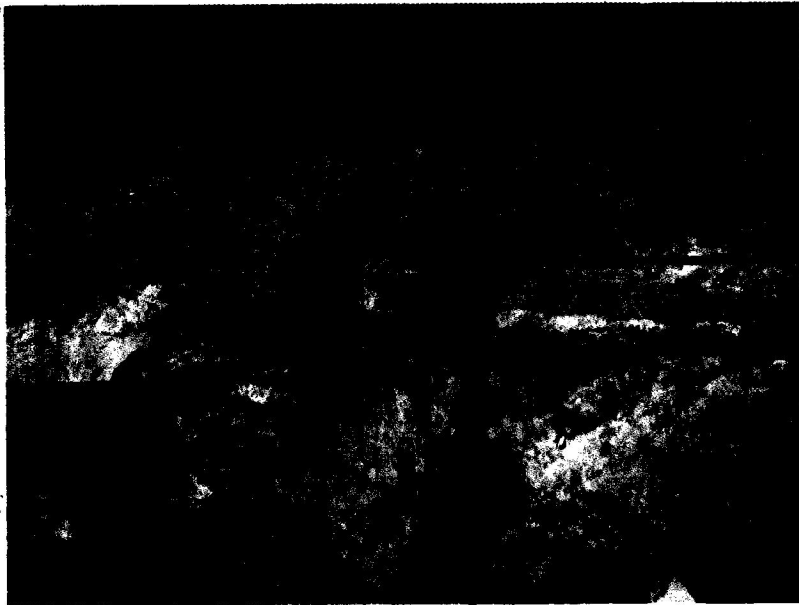


**Fig. 4.6:** A medium bedded ironstone of the Bende-Ameki Formation. Note that the red lines mark out the ironstone bed.



## **4.2 Sedimentary Structures**

Some structures were recorded in the lithologic section of the study area. These structures include; planar cross stratification and herringbone cross stratification. Planar cross stratification was observed on two sandstone beds OS10 and OS12, while herringbone cross stratification was observed on sandstone bed OS13. Other structure includes lamination in shale which must have occurred as a result of influx of other sediments during the period of the shale deposition.

### **4.2.1 Planar cross stratification**

Planar cross stratifications are cross beddings that are inclined at an angle to both lower and upper bedding plane within a single bed (Fig. 4.7). The planar cross stratification implies that the sandstone must have formed on point bars in the lower flow regime (shallow stream) which is likely to be a braided river environment. The fluvial origin is supported by unidirectional paleocurrent pattern and absence of marine biogenic features (Ojo & Akande, 2003; Rust & Jones, 1987)

### **4.2.2 Herringbone cross stratification**

Herringbone cross stratification was observed on one of the sandstone beds. It has a bidirectional structure like that of a fishbone (Fig. 4.8). This structure suggests a change in flow direction during the time of deposition. The herringbone cross stratified sandstone subfacies is interpreted as tidal channel facies. Klein (1970) suggested that current direction reversals are associated with tidal processes.



**Fig. 4.7:** Planar cross stratified medium grained sandstone showing an inclined unidirectional structure

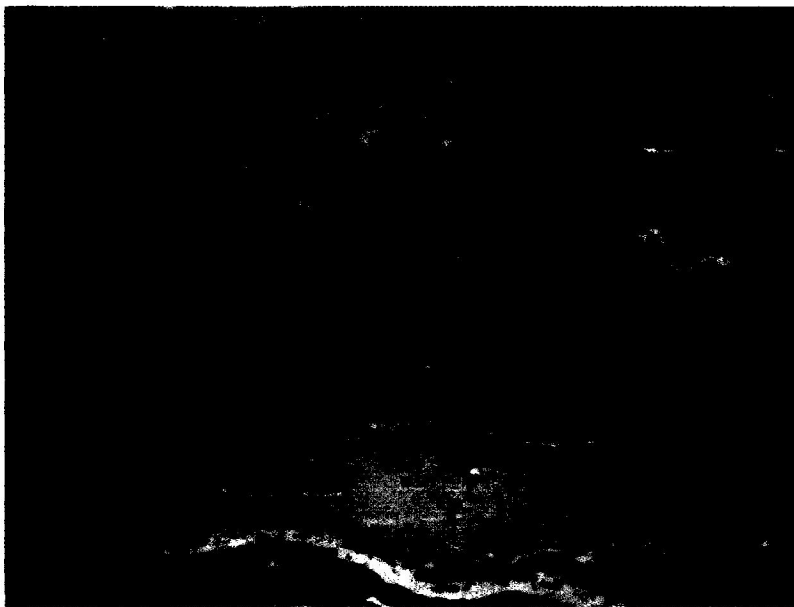


**Fig. 4.8:** Ferruginized herringbone cross stratified medium grained sandstone showing an inclined unidirectional structure

### 4.3 Grain Size Analysis

Five sandstone samples were analysed to derive grain size distribution (Tables 4.1 – 4.5). The results obtained were used in plotting graphs of cumulative weight retained (%) against phi size (Fig. 4.9 - 4.13). The data derived from the graph plotted was used to calculate the graphic mean, graphic standard deviation (sorting), graphic skewness and graphic kurtosis based on Folk and Ward, 1957 formula (Appendix I). The mean size of the samples ranges from 0.88 to 1.87 $\Phi$  with an average value of 1.36 $\Phi$  suggesting that the samples are predominantly medium grained sand (Appendix II). The sorting values range from 0.64 to 0.95 $\Phi$  with an average value of 0.82 $\Phi$  suggesting that the sandstone samples are essentially moderately sorted. More so, the skewness values range from -0.337 to 0.17 with an average value of -0.038. This suggests that the sandstone samples are near symmetrical. Kurtosis values range from 0.98 to 1.72 with an average value of 1.32 suggesting that the samples are essentially leptokurtic (Table 4.6).

The Bende-Ameki sandstones are essentially moderately sorted sand which is similar to those obtained from fluvial sands (Folk, 1974). The plots of skewness against standard deviation, and mean against standard deviation reveal that the sandstones of the study area are fluvial (Fig. 4.14).

**Table 4.1:** Grain size data for sample OS10

S/N	Sieve size (mm) (d)	Phi ( $\Phi$ ) = $-\log_2 d$	weight retained (g)	Individual weight retained (%)	Cumulative weight retained (g)	Cumulative weight retained (%)
1	4.000	-2.0	0.3	0.3	0.3	0.3
2	3.350	-1.7	0.1	0.1	0.4	0.4
3	2.000	-1.0	0.6	0.6	1	1
4	1.180	-0.2	0.8	0.8	1.8	1.8
5	0.600	0.7	15.9	15.9	17.7	17.7
6	0.400	1.2	21.7	21.7	39.4	39.4
7	0.150	2.7	58.9	59	98.3	98.4
8	0.075	3.7	1.5	1.5	99.8	99.9
9	0.063	4.0	0.1	0.1	99.9	100

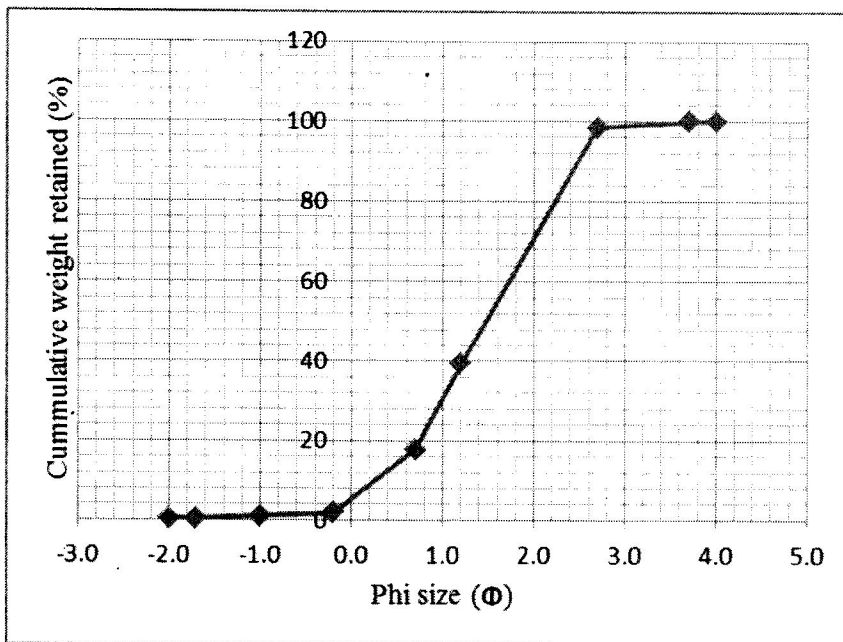


**Fig. 4.9:** Graph of grain size distribution for sample OS10.

**Table 4.2:** Grain size data for sample OS11

S/N	Sieve size (mm) (d)	Phi ( $\Phi$ ) = $-\log_2 d$	weight retained (g)	Individual weight retained (%)	Cumulative weight retained (g)	Cumulative weight retained (%)
1	4.000	-2.0	0.1	0.1	0.1	0.1
2	3.350	-1.7	0.3	0.3	0.4	0.4
3	2.000	-1.0	2.7	2.7	3.1	3.1
4	1.180	-0.2	3.8	3.7	6.8	6.9
5	0.600	0.7	6.9	6.8	13.6	13.8
6	0.400	1.2	3.3	3.3	16.9	17.1
7	0.150	2.7	74.1	75.2	91	92.3
8	0.075	3.7	7.2	7.3	98.2	99.6
9	0.063	4.0	0.4	0.4	98.6	100

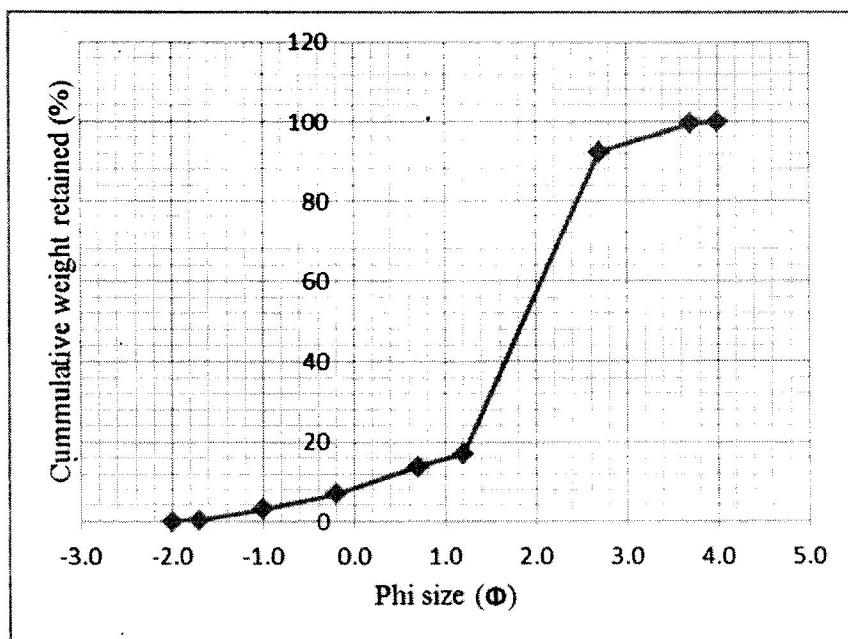


**Fig. 4.10:** Graph of grain size distribution for sample OS11.

**Table 4.3: Grain size data for sample OS12**

S/N	Sieve size (mm) (d)	Phi ( $\Phi$ ) = $-\log_2 d$	weight retained (g)	Individual weight retained (%)	Cumulative weight retained (g)	Cumulative weight retained (%)
1	4.000	-2.0	0.6	0.6	0.6	0.6
2	3.350	-1.7	0.6	0.6	1.2	1.2
3	2.000	-1.0	3.5	3.5	4.7	4.7
4	1.180	-0.2	3.8	3.8	8.5	8.5
5	0.600	0.7	22.4	22.5	30.9	31
6	0.400	1.2	19.1	19.2	50	50.2
7	0.150	2.7	46.5	46.8	96.5	97
8	0.075	3.7	2.7	2.7	99.2	99.7
9	0.063	4.0	0.2	0.2	99.4	99.9

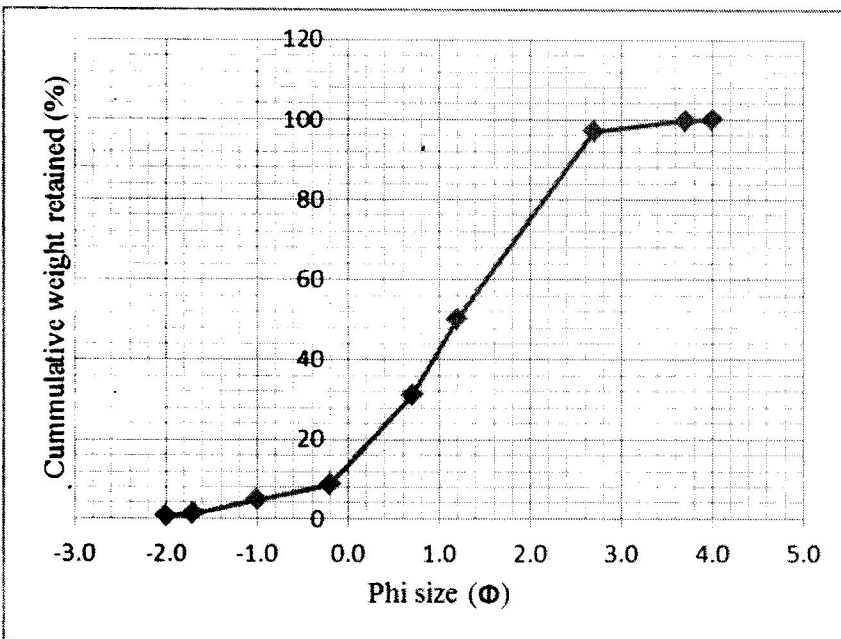


**Fig. 4.11: Graph of grain size distribution for sample OS12.**

**Table 4.4:** Grain size data for sample OS13

S/N	Sieve size (mm) (d)	Phi ( $\Phi$ ) = $-\log_2 d$	weight retained (g)	Individual weight retained (%)	Cumulative weight retained (g)	Cumulative weight retained (%)
1	4.000	-2.0	0	0	0	0
2	3.350	-1.7	0	0	0	0
3	2.000	-1.0	0.1	0.1	0.1	0.1
4	1.180	-0.2	0.4	0.4	0.5	0.5
5	0.600	0.7	14.9	14.9	15.4	15.4
6	0.400	1.2	42.5	42.6	57.9	58
7	0.150	2.7	40.4	40.5	98.3	98.5
8	0.075	3.7	1.4	1.4	99.7	99.9
9	0.063	4.0	0.1	0.1	99.8	100

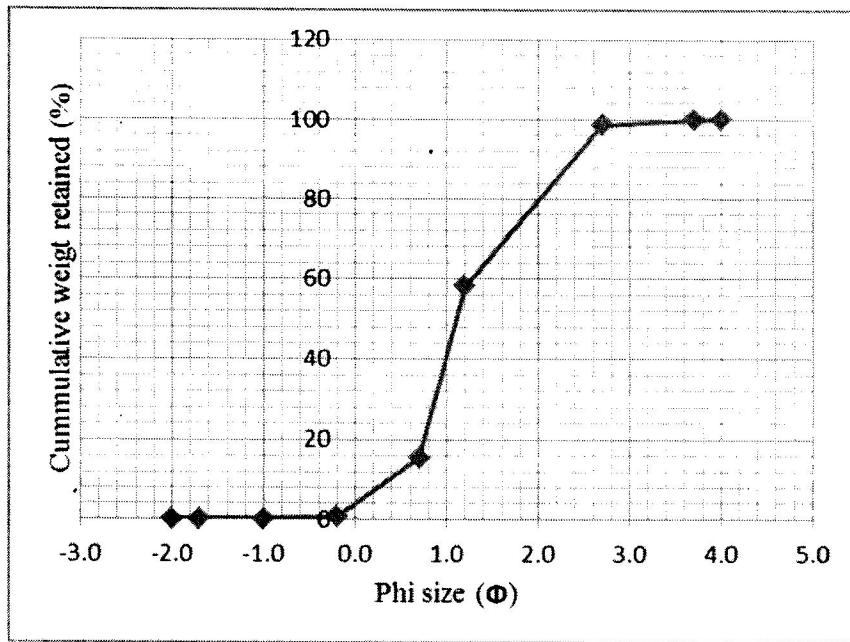


**Fig. 4.12:** Graph of grain size distribution for sample OS13.

**Table 4.5:** Grain size data for sample OS14

S/N	Sieve size (mm) (d)	Phi ( $\Phi$ ) = $-\log_2 d$	weight retained (g)	Individual weight retained (%)	Cumulative weight retained (g)	Cumulative weight retained (%)
1	4.000	-2.0	0	0	0	0
2	3.350	-1.7	0	0	0	0
3	2.000	-1.0	0.9	0.9	0.9	0.9
4	1.180	-0.2	2.7	2.7	3.6	3.6
5	0.600	0.7	36	36.1	39.6	39.7
6	0.400	1.2	30.9	31	70.5	70.7
7	0.150	2.7	25.5	25.6	96	96.3
8	0.075	3.7	3.4	3.4	66.4	99.7
9	0.063	4.0	0.3	0.3	99.7	100

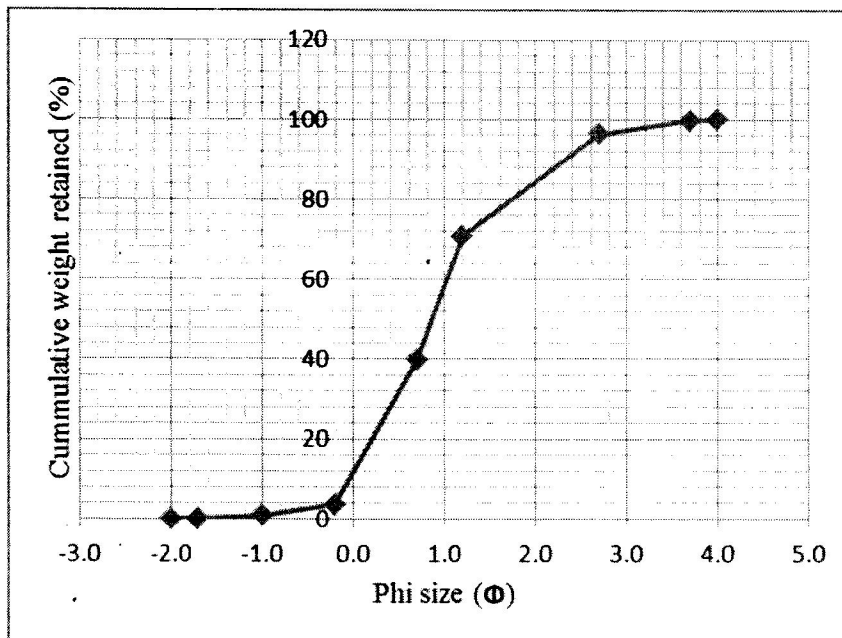


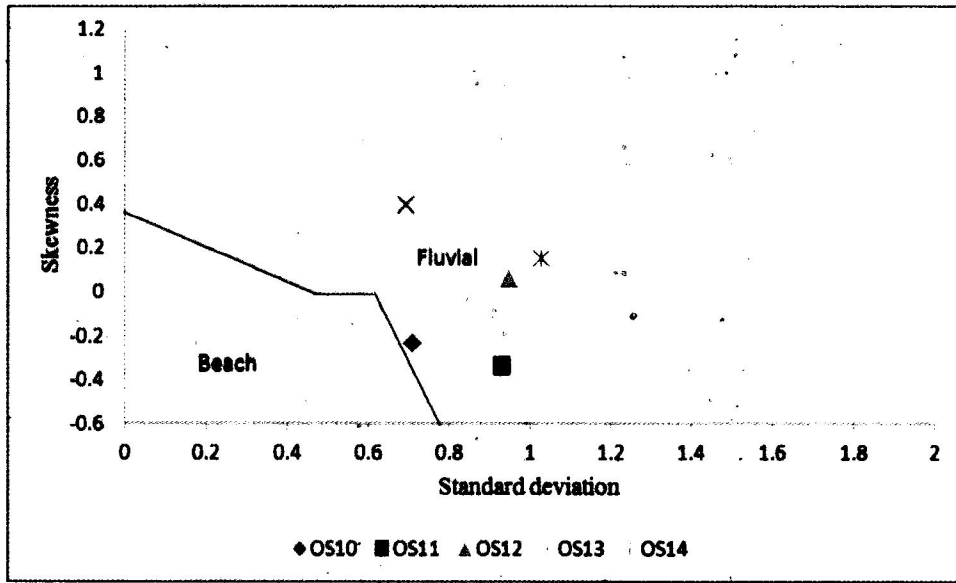
**Fig. 4.13:** Graph of grain size distribution for sample OS14.



**Table 4.8:** Grain size analysis interpretation

S/N	Result					Interpretation			
	Sample no.	Graphic mean	Sorting	Skewness	Kurtosis	Graphic mean	Sorting	Skewness	Kurtosis
1	OS 10	1.4	0.71	-0.232	0.98	Medium sand	Moderately well sorted	Coarse skewed	Mesokurtic
2	OS 11	1.87	0.93	-0.337	1.9	Medium sand	Moderately sorted	Strongly coarse skewed	Very leptokurtic
3	OS 12	1.4	0.95	0.06	0.99	Medium sand	Moderately sorted	Near symmetrical	Mesokurtic
4	OS 13	1.24	0.64	0.17	1.72	Medium sand	Moderately well sorted	Fine skewed	Very leptokurtic
5	OS 14	0.88	0.85	0.15	1.03	Coarse sand	Moderately sorted	Fine skewed	Mesokurtic
	<b>Average</b>	1.36	0.82	-0.038	1.32	Medium sand	Moderately sorted	Near symmetrical	Leptokurtic

(A)



(A)

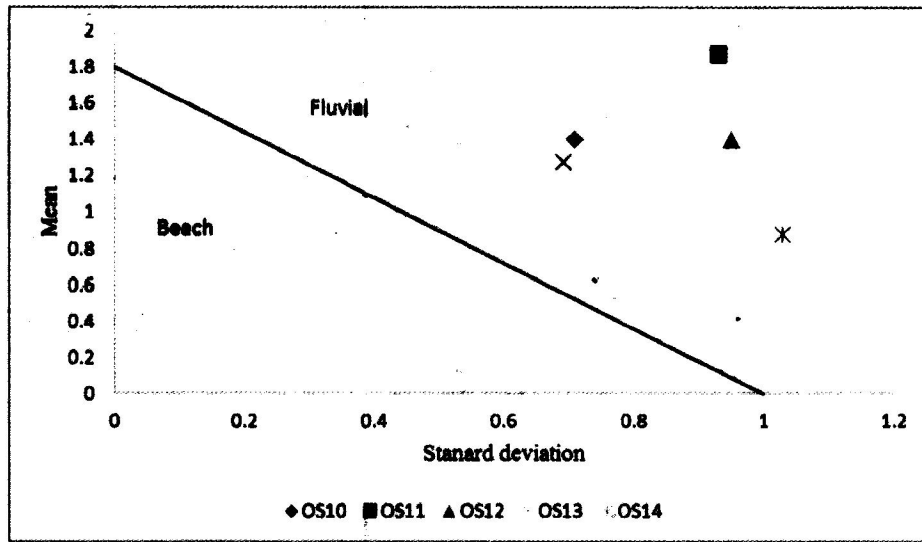


Fig 4.14: Scatter plot of (A) skewness against standard deviation, (B) mean against standard deviation (after Friedman, 1967).

## 4.4 Petrography

### 4.4.1 Mineralogy

Petrographic analysis was carried out on six sandstone samples to determine the quantitative mineralogical compositions. The conventional petrographic microscope shows the mode of occurrence of individual constituents, cementing materials and their relative abundance. Quartz, feldspar, mica, clay minerals, rock fragments and cementing materials are the primary constituents of sandstone (Table 4.7).

Quartz which is the most common rock forming mineral because of its resistance to weathering occurs as the main component of the sandstones. It shows first order grey to white-yellow, low birefringence, low relief, lacks cleavage and shows extinction under cross polarized light. It is the most common mineral constituent of the sandstones with relative abundance ranging from 53% to 70% and average abundance of 63% (Table 4.7). The sandstones consist both monocrystalline and polycrystalline quartz. If it has one crystal in a grain then it is monocrystalline, but if it has more than one crystal within a grain then it is polycrystalline (Fig. 4.15 – 4.17). The clear non-undulous feature suggests that the quartz is derived from an igneous source rock (Basu, 1985). Some of the quartz grain appears to be stained with brownish colours which must have been as a result of ferruginization (Fig. 4.15). Feldspar displays low relief, low birefringence with first order white to grey colour. They are recognized by the presence of their twining under cross polarized light which is either lamellar (microcline feldspar) or cross hatch (plagioclase feldspar). The microcline feldspar is the most occurring feldspar in the sandstone samples (Fig. 4.15 and Fig. 4.17) constituting 6% to 14% with an average of 9.8% of the total constituent. The microcline feldspars indicate a slow cooling process which is the characteristics of plutonic rocks.

Mica is a minor component of the sandstone samples with relative abundance of 1% to 4% with an average value of 3% (Table 4.7). The micas occur as prismatic, tabular or elongated minerals, and they which show moderate relief, parallel extinction and have greenish third order interference colour (Fig. 4.16).

Other constituents include Clay matrix (Fig. 4.16) with relative abundance of 5% to 10%. They may have formed from the chemical decomposition of feldspar. Rock fragments have relative abundance of 2% to 12%, and may have formed from pre-existing igneous, metamorphic or sedimentary rock. Goethites have relative abundance of 4% to 15% and may have formed as a result of oxidation of the sandstones (Fig. 4.16).

**Table 4.7:** Quantitative mineralogical composition of sandstones of the Bende-Ameki Formation

S/N	Sample number	Monocrystalline Quartz (%)	Polycrystalline Quartz (%)	Total Quartz (%)	Plagioclase Feldspar (%)	Microcline Feldspar (%)	Total Feldspar (%)	Mica (%)	Clay Matrix (%)	Rock fragment (%)	Goethite (%)
1	OS06	37	16	53	5	14	19	4	10	8	6
2	OS10	58	12	70	3	10	13	2	6	4	5
3	OS11	37	29	66	4	10	14	3	5	8	4
4	OS12	41	14	55	3	10	13	4	9	12	7
5	OS13	41	20	61	3	9	12	1	7	4	15
6	OS14	51	19	70	2	6	8	4	6	2	10



**Fig 4.15:** Photomicrograph of sandstone sample OS 13 showing the mineralogical composition and texture under cross polar. Note the presence of Monocrystalline Quartz (MQ) and Microcline Feldspar (MF).

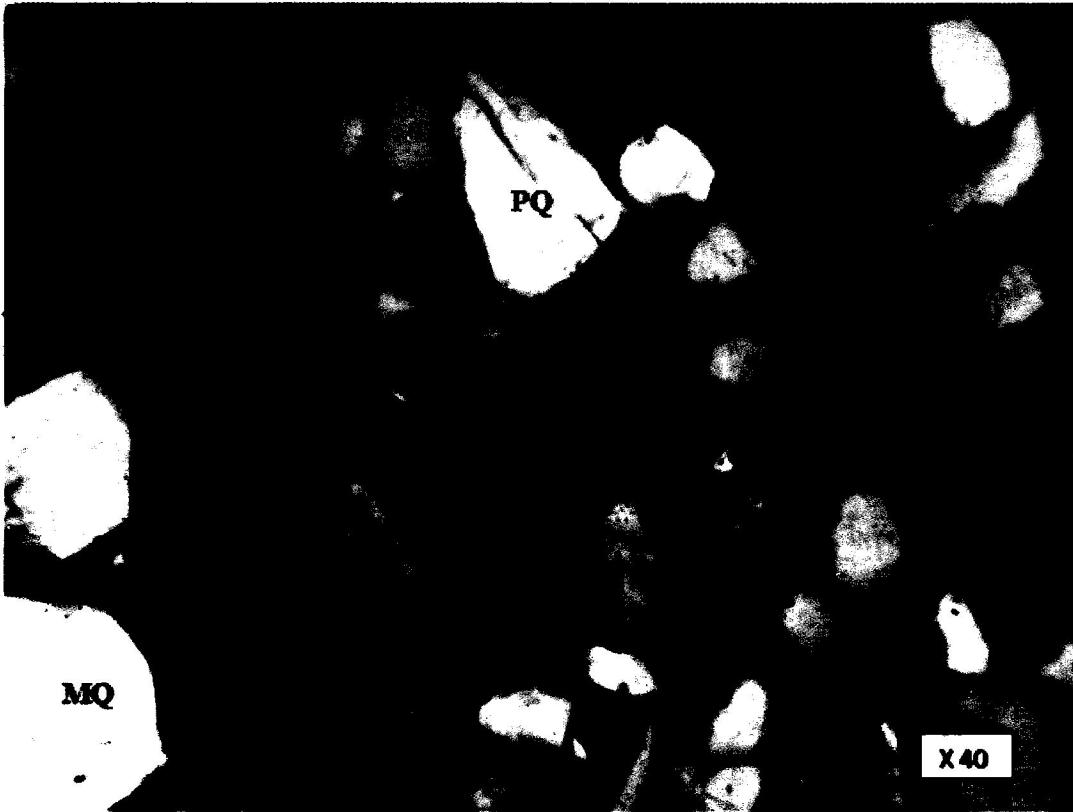


**Fig 4.16:** Photomicrograph of sandstone sample OS 06 showing the mineralogical composition and texture under cross polar. Note the presence of Monocrystalline Quartz (MQ), Mica (M), Goethite (G), and of Clay matrix (C).

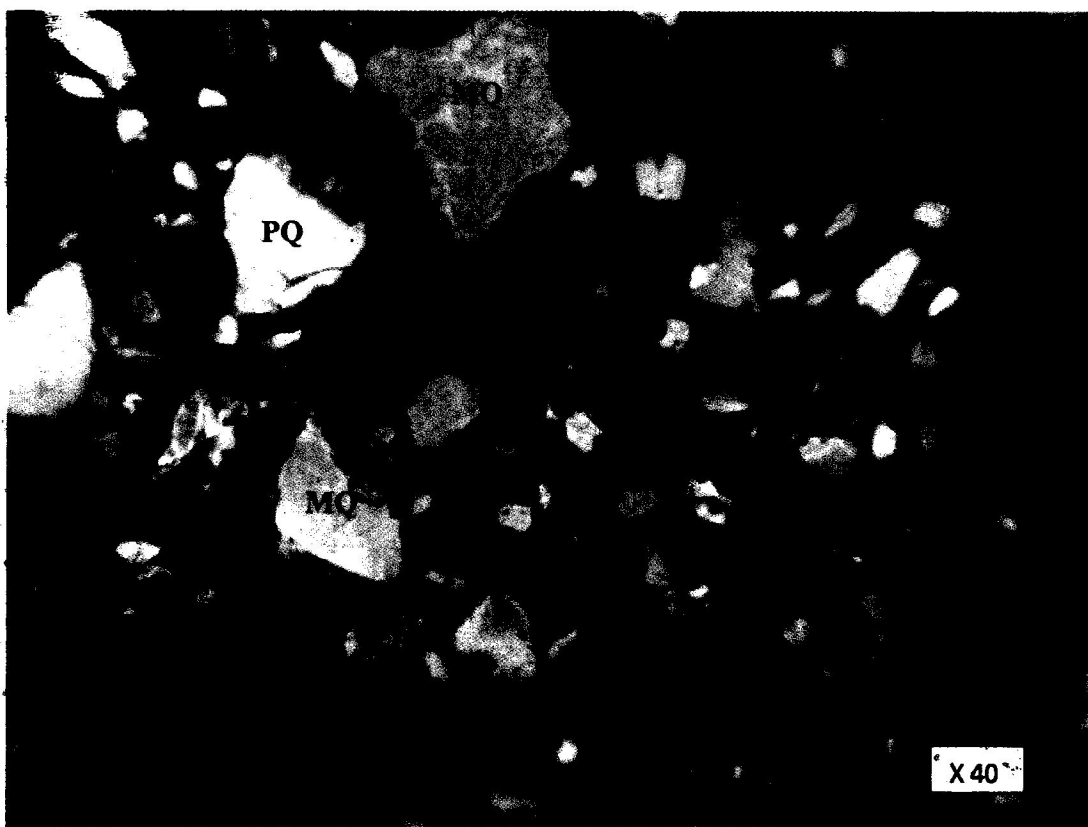


**Fig 4.17:** Photomicrograph of sandstone sample OS 14 showing the mineralogical composition and texture under cross polar. Note the presence of Monocrystalline Quartz (MQ), Polycrystalline Quartz (PQ) and Microcline Feldspar (MF).

#### 4.4.2 Classification of the Sandstones

The major framework components of sandstone (quartz, feldspar and rock fragments) were recalculated to 100% (Table 4.8) for QFR ternary diagram allowing them to occupy one of the poles according to the scheme of Folk (1974). The modal analysis of the sandstones shows that the samples have abundant quartz which ranges from 66-88% with an average value of 76.2%. The feldspars ranging from 10-24% in relative abundance with an average value of 16%, while the rock fragments ranges in relative abundance from 2-15% with an average value of 8%. The ternary diagram plotted from the values of the major framework components of the sandstones classifies the sandstones of the Bende-Ameki Formation into subarkose and lithic subarkose (Fig. 4.18).

**Table 4.8:** Relative abundance of sandstone framework components

S/N	Sample number	Location	Quartz (%)	Feldspar (%)	Rock fragments (%)
1	OS06	Onitsha-Awka	66	24	10
2	OS10	Onitsha-Awka	80	15	5
3	OS11	Onitsha-Awka	75	16	9
4	OS12	Onitsha-Awka	69	16	15
5	OS13	Onitsha-Awka	79	16	5
6	OS14	Onitsha-Awka	88	10	2



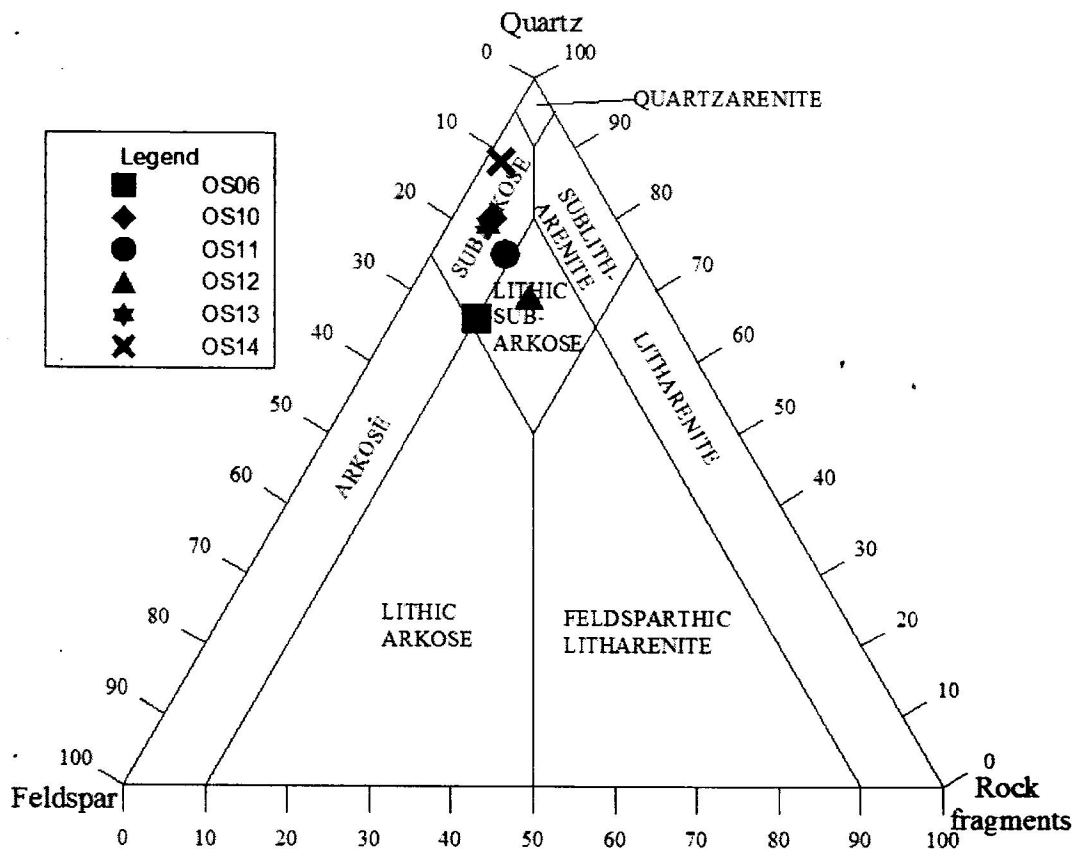


**Fig. 4.18:** Ternary plots for the classification of sandstones of the Bende-Ameki Formation (after Folk, 1974)

## 4.5 Organic Geochemistry

Five (5) shale samples were evaluated by Rock Eval Pyrolysis to determine the organic richness and quality of the organic matter in the rocks. The Rock Eval data are presented on Table 4.9 with the geochemical parameters.

**Table 4.9:** Data derived from Rock Eval Pyrolysis.

S/N	Sample No.	Lithology	TOC (wt %)	S1 (mgHC/g rock)	S2 (mgHC/g rock)	S3 (mgHC/g rock)	GP (S1+S2) (mgHC/g rock)	T <sub>max</sub> °C	HI (mgHC/g TOC)	OI (mg/g)	PI
1	OS 01	Shale	2.25	0.17	1.86	0.37	2.03	424	83	16	0.08
2	OS 03	Shale	0.46	0.07	0.39	0.34	0.46	424	84	74	0.15
3	OS 05	Shale	5.08	0.99	8.04	1.57	9.03	431	158	31	0.11
4	OS 07	Shale	3.27	0.48	3.75	0.88	4.23	427	115	27	0.11
5	OS 17	Shale	1.73	0.14	1.36	0.45	1.5	427	79	26	0.09

### 4.5.1 Total Organic Carbon (TOC)

TOC of five shale samples from the study area ranges from 0.46 - 5.08wt% with an average TOC value of 2.56wt%. OS01 has TOC value of 0.46wt% indicating a poor source rock, while other samples have TOC greater than 0.5wt% and such levels of organic enrichment are considered as good source rocks for hydrocarbon generation (Peters and Cassa, 1994).

### 4.5.2 Hydrogen Index (HI)

Although organic matter content in sediments is usually estimated by a determination of organic carbon, the limiting element in the petroleum forming reaction is not carbon but hydrogen. The reason for analysing carbon, however, is that only the hydrogen bonded in organic molecules is active in the petroleum forming processes.

The HI values of all the samples ranges from 79 to 158mgHC/gTOC with an average value of 103.8 mgHC/gTOC, indicating that the shales are of Type III gas prone kerogen. The production of these hydrocarbons by pyrolysis is linked to the amount of hydrogen the rock contains.

### 4.5.3 Thermal Maturity

T<sub>max</sub> value represents the temperature at which the largest amount of hydrocarbons is produced in the laboratory during pyrolysis. The thermal maturation level can be estimated from the T<sub>max</sub> values. T<sub>max</sub> of the Bende-Ameki shales ranges from 424°C - 431°C (mean = 426.6°C). This indicates that the shales of Bende-Ameki Formation are thermally immature.

### 4.5.4 Generative Potential

To further highlight the source rock potential of the sediments, the generative potential (GP = S<sub>1</sub>+S<sub>2</sub>) is used. Rocks having GP value < 2mg HC/g rock corresponds to gas prone rocks or non-generative rock, rocks with GP between 2 and 6mg HC/g rock are moderate source rocks and those with GP > 6mg HC/g rock are good source rocks (Peters and Cassa, 1994; Tissot and Welte, 1984). Rock-Eval Pyrolysis results showed that the shales have GP values ranging from 0.46 to 9.03mg HC/g rock with an average value of 3.45mg HC/g rock. This result supports the HI result that the shales are gas prone (Peters and Cassa, 1994).

### 4.5.5 Kerogen Type

Kerogens are constituent of the sedimentary rocks that is neither soluble in aqueous alkaline solvents nor in the common organic solvents. Kerogen is the most important form of organic carbon on earth and represents usually from 80 to 99% of the organic matter, the rest being bitumen (Tissot and Welte 1984). Cross plot of the Hydrogen Index (HI) versus T<sub>max</sub> shows that majority of the samples plot within Types III gas prone kerogen (Fig. 4.19).

The graph of Hydrogen Index (HI) against Oxygen (OI) shows that the organic matter contained in the sediments are predominantly the Type II and Type III which are oil and gas prone and gas prone respectively (Fig. 4.20). Plot of S<sub>2</sub> against TOC for the sediments indicates that they are capable of generating gas (Fig. 4.21). Four of the shale samples are capable of generating gas while one of the samples (OS03) is organically lean. Plots of PI versus T<sub>max</sub> further shows that sediments are predominantly within the immature window in the stained or contaminated phase with respect to hydrocarbon generation (Fig. 4.22).

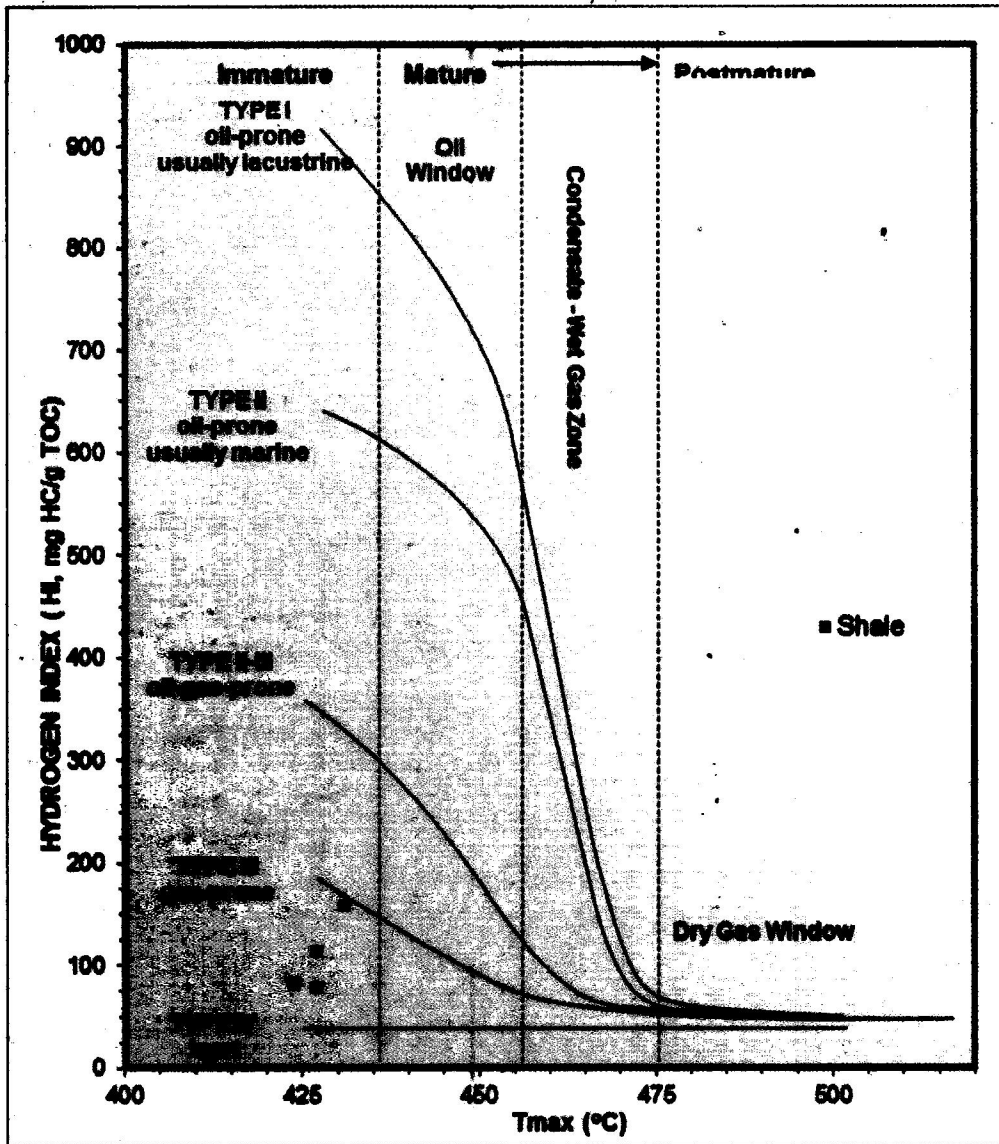


Fig. 4.20: Graph of Hydrogen Index(HI) against Tmax.

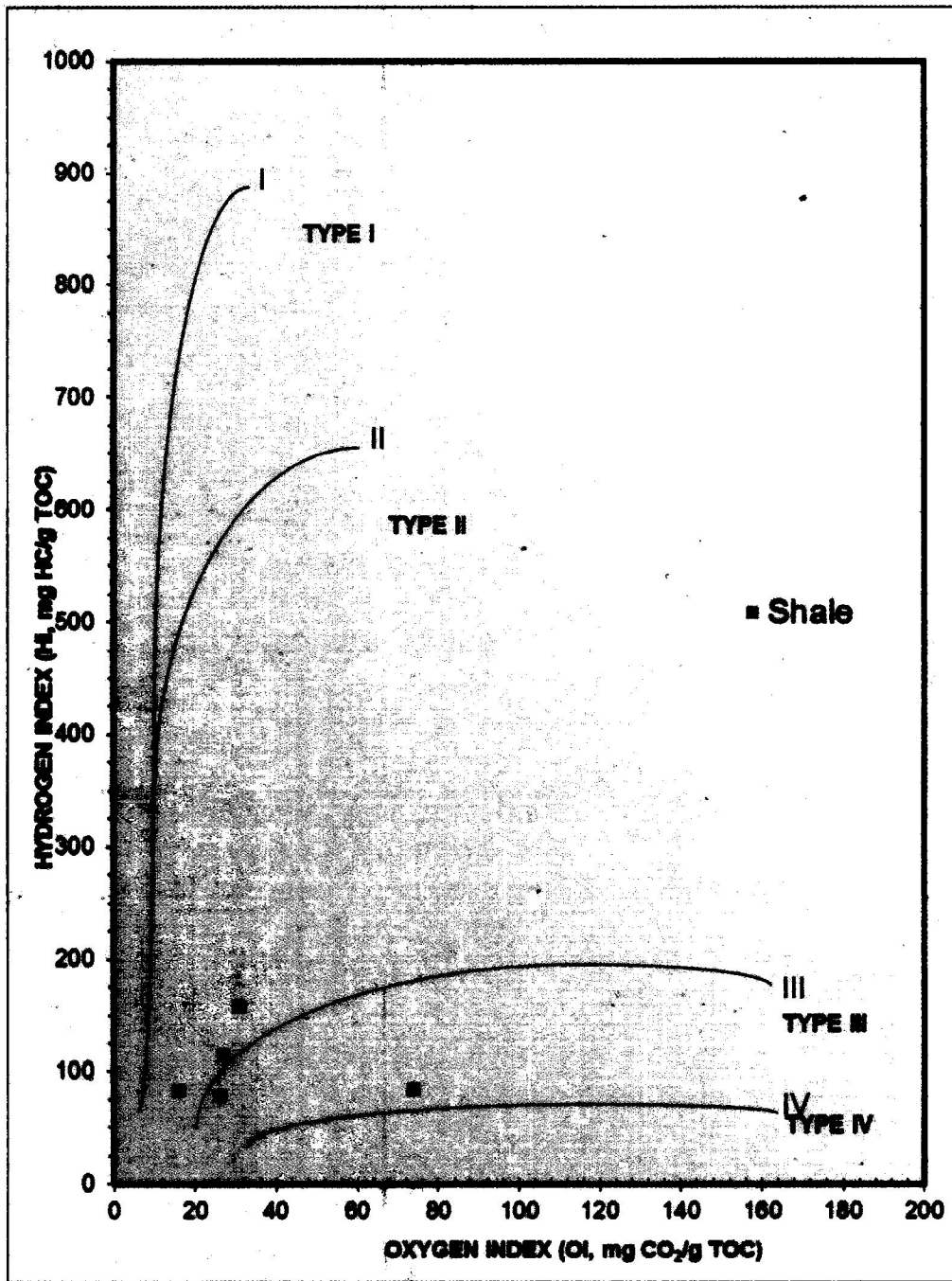


Fig 4.21: Graph of Hydrogen Index (HI) against Oxygen Index (OI).

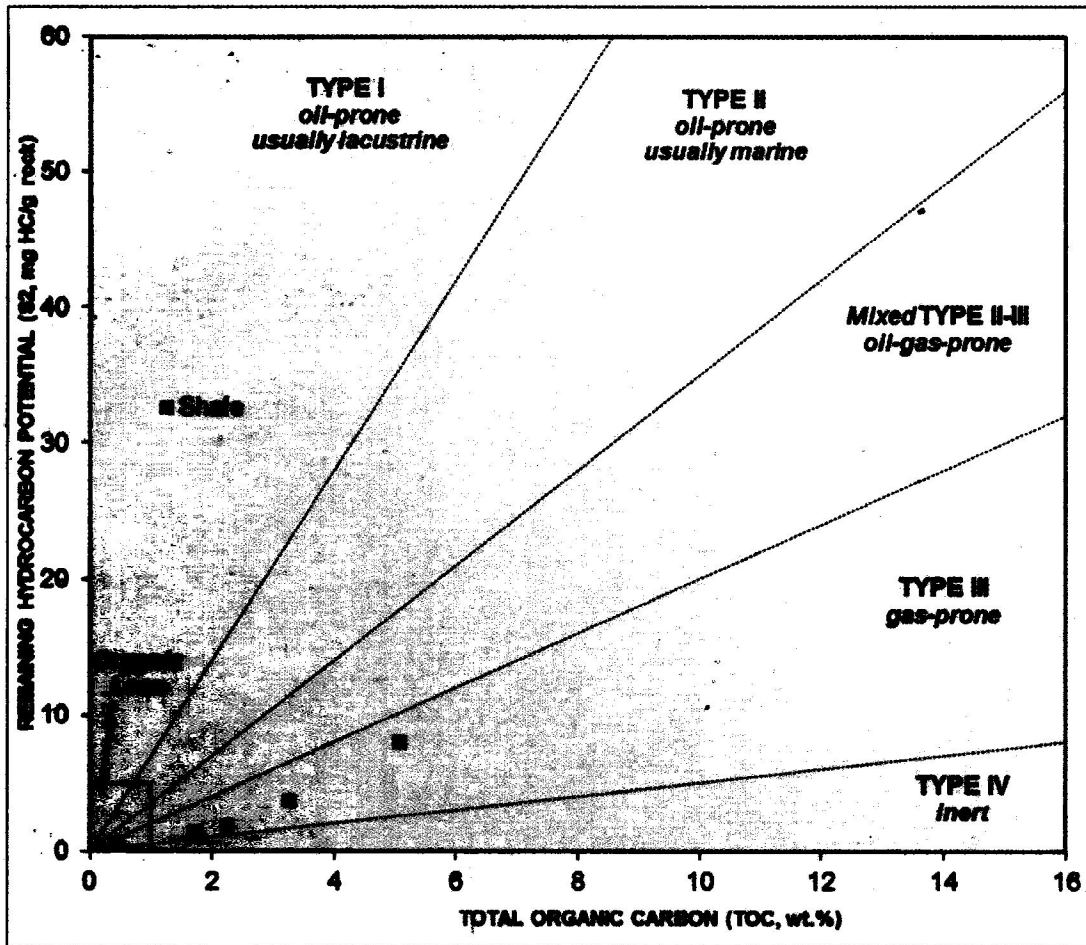


Fig. 4.22: Graph of S2 against TOC.

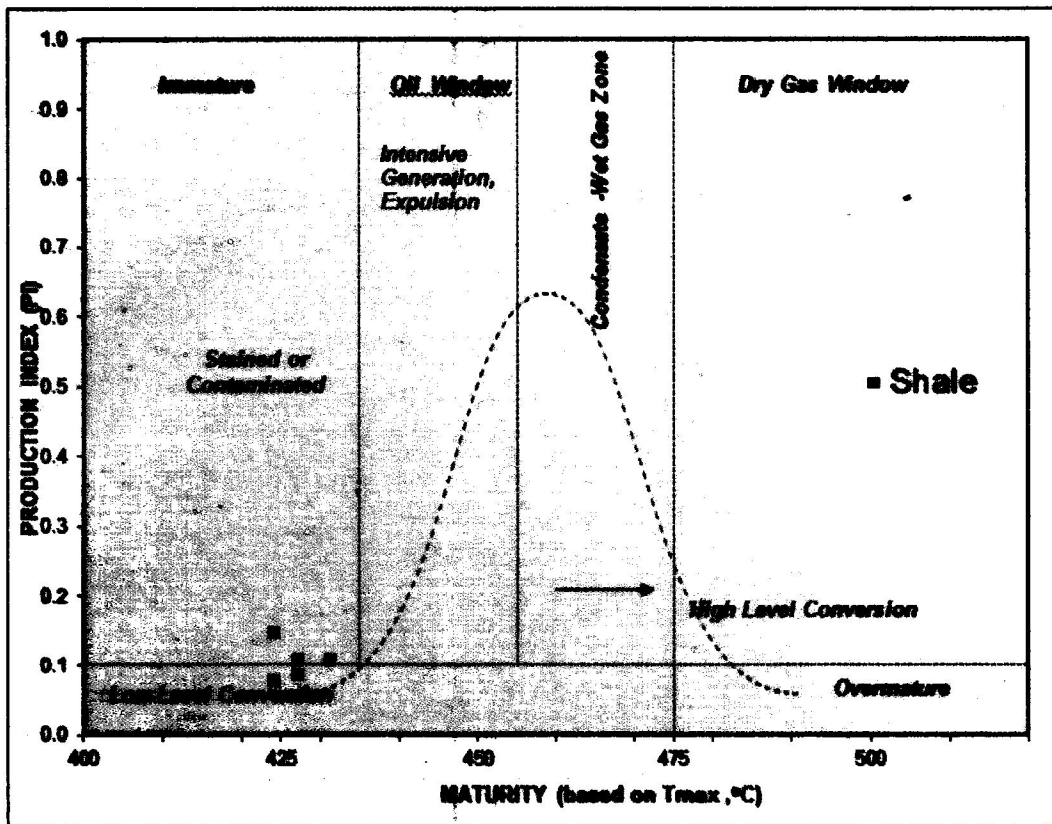


Fig. 4.22: Graph of PI against  $T_{max}$ .

## CHAPTER FIVE

### CONCLUSIONS

#### 5.1 Conclusions

The Eocene Bende-Ameki Formation exposed at the Onitsha-Awka express road in the Anambra Basin is composed of shale, ironstone, sandstone, claystone, and siltstone facies. The Formation was studied in order to determine the environment of deposition and the petroleum potential. The study concluded at the following;

Granulometric analysis suggests that the sandstone are medium grained, moderately sorted, near symmetrical and leptokurtic which suggests that the sandstone were deposited in a fluvial environment. Scatter plots of skewness against standard deviation and mean against standard deviation likewise confirmed that the sandstones of the study area are predominantly fluvial.

The dominance of quartz greater than 75% in the petrographic analysis suggests that the sandstones are mineralogically mature. The QFR ternary diagram plotted from the values of the major framework components of sandstones reveals that the sandstones of the Bende-Ameki Formation are essentially subarkose to lithic subarkose.

Source rock studies on the shales have good organic matter content and can therefore be considered as potential petroleum source rocks which upon thermal maturity would produce gas.



## REFERENCES

- Abubakar, M. B., 2014. Petroleum Potential of the Nigerian Benue Trough and Anambra Basin: A Regional Synthesis. *Journal of Scientific Research: Natural Resources*, Vol. 5(1), Article ID: 42533, pp. 34.
- Adegoke, O. S., 1969. Eocene Stratigraphy of Southern Nigeria. *Bull. Bur. Rech. Geo Min Memoir* 69, pp. 22-48.
- Adegoke, O. S., Ako B. D. and Enu E. I., 1980. Geotechnical Investigation of Ondo State Bituminous Sands. Geology and Reserve Estimate. Rept. Geological Consulting Unit, Department of Geology, University of Ife, Vol. 1, pp. 257.
- Adeoye, M.O., Ndeze, C. k., Akande, S. O. and Ojo, O. J., 2016a. Petrographic Facies Evaluation, Provenance and Depositional Environment of the Oligocene – Miocene Ogwashi Asaba Formation, Southern Anambra Basin, Nigeria. *Journal of Mining and Geology*, Vol. 52(1), pp. 1-18
- Adeoye, M.O., Ndeze, C. k., Akande, S. O. and Ojo, O. J., 2016b. Foraminifera and Paleoenvironment of the Tertiary Ogwashi Asaba Formation, Southern Anambra Basin, Nigeria. *Proceedings of the 2016 Faculty of Science International Conference*, Department of Geology, Federal University Oye-Ekiti, Oye-Ekiti, Ekiti State, Nigeria. pp. 100 – 102.
- Akaegbobi, I. M., Nwachukwu, J. I., and Schmitt, M., 2000. Aromatic Hydrocarbon Distribution and Calculation of Oil and Gas Volumes in Post-Santonian Shale and Coal, Anambra Basin, Nigeria: In M. R. Bello and B. J. Katz, eds., *Petroleum Systems of South Atlantic Margins: Amer. Assoc. Petrol. Geol. Memoir* 73, pp. 233-245
- Akande, S. O., Adekeye, O. A., Ojo, O. J., Lewan, M., Pawlewicz, M., Egenhoff, S. and Samuel, O., 2010. Comparison of Hydrous Pyrolysis Petroleum Yields and Composition from Nigerian Lignite and Associated Coaly Shale in the Anambra Basin: *Search and Discovery Article #40647*.
- Akande, S. O., Egenhoff, S. O., Obaje, N. G., Ojo, O. J., Adekeye, O. A. and Erdtmann B. D., 2012. Hydrocarbon Potential of Cretaceous Sediments in the Lower and Middle Benue Trough, Nigeria: Insights from New Source Rock Facies Evaluation: *Journal of African Earth Sciences*, Vol. 64, pp. 34-47.

- Akande, S. O., Ojo, O. J. and Dekeye, O. A., 2011, Stratigraphic Evolution and Petroleum potential of Middle Cretaceous Sediments in Lower Benue and Middle Benue Trough, Nigeria; Insight from New Sorce Rock Faxies Evaluation, *Petrol. Technol. Dev. J.*, pp. 11 – 34.
- Arua, I., 1980. Palaeocene Macrofossils from the Imo Shale in Anambra Basin, Nigeria. *Journal of Mining and Geology*, Vol. 17, pp. 81– 84.
- Arua, I., 1986. Paleoenvironment of Eocene Deposits in the Afikpo Syncline, Southern Nigeria. *Journal Of African Earth Sciences*, Vol. 5, pp. 279-284.
- Avbovbo, A. A., Ayoola, E. O. and Osahon, G. A., 1986. Depositional and Structural Style in Chad Basin of Northeastern Nigeria. *AAPG Bulletin*, Vol. 70(12), pp. 1787-1798.
- Basu, A., 1985. Influence of Climate and Relief of Compositions of Sand Related at Source Areas. In: *Provenance of Arenites*, G. G. Zuffa (ed.), NATO-ASI, V.C-148, Reidei, Holldel, pp. 1-18
- Benkhelil, J., 1986. Carateristiques Structurales et Evolution Geodynamique du Basin Intra – Continental de la Benoue" Nigeria : These d"etat, Nice, pp. 275.
- Berggren, W. A., 1960. Paleocene Biostratigraphy and Planktonic Foraminifera of Nigeria (West Africa). *International Geological Congress, Copenhagen, Report*, Vol. 21(6), pp. 41-55.
- Burke, K. C., Desauvagie, T. F. J. and Whiteman, A. J., 1971. Opening of the Gulf of Guinea and Geological history of the Benue Depression and Niger Delta. *Nature*, Vol. 233, pp. 51-55.
- Burke, K. C., Dewey, J. F., 1972. Orogeny in Africa. In: *Dessauvagie TFJ, Whiteman AJ (eds), Africa Geology*. University of Ibadan Press, Ibadan, pp. 583–608
- Fayose, E. A. and Ola, P. S. 1990. Radiolarian Occurences in the Ameki Type Section, Eastern Nigeria. *Journal of Mining and Geology*, Vol. 26, pp. 75-80.
- Folk, R. L. and Ward, W., 1957. Brazes River Bar; A study of the Significance of Grain Size Parameters. *Journal of Sedimentary Petrology*, Vol. 27, pp. 3-26.
- Folk, R. l., 1974. *Petrology of Sedimentary Rocks*; Hemphill, Austin Texas, pp. 3-26

- Friedman, G. M., 1967. Dynamic Processes and Statistical Parameters Compared for Size Frequency Distinction of Beach and River Sands: *Journal of Sedimentary Petrology*, Vol. 37, pp. 327-354.
- Jan du CheˆNe RE, De Klasz I, Archibong, E. E., 1979. Biostratigraphic Study of the Borehole Ojo-1, SW Nigeria, with Special Emphasis on the Cretaceous Microflora. *Revue de Micropalaeontologie* Vol. 21, pp. 123–139
- Klein, G. D., 1970. Depositional and Dispersal Dynamics of Intertidal Sand Bars. *Jour. Sedimentary Petrology*, Vol. 40, pp. 1095 – 1127.
- Kogbe, C. A., 1976. Paleogeographic History of Nigeria from Albian Times. In: Kogbe, C.A. (Ed.), *Geology of Nigeria*. Elizabethan Publishers, Lagos, pp. 237–252
- Kogbe, C. A., 1989. *Geology of Nigeria*, 2nd Edition. Rockview Nigeria Limited, Jos, pp. 538
- Ladipo, K. O., Nwajide, C. S. and Akande, S. O., 1992. Cretaceous and Paleogene Sequences in the Abakaliki and Anambra Basins, Southeastern Nigeria, National Symposium on Geology of deltas.
- Murat, R. C., 1970. Stratigraphy and Paleogeography of the Cretaceous and Lower Tertiary in Southern Nigeria. In: Dessauagie, F. J. and Whiteman, A. J. (Ed). *African Geology*, University of Ibadan Press, Ibadan, Nigeria, pp. 251 – 266.
- Nwachukwu, J. I., 1972. The Tectonic Evolution of the Southern Portion of the Benue Trough, Nigeria. *Geology Magazine*, Vol. 109, pp. 511-419
- Nwajide, C. S., 1990. Cretaceous Sedimentation and Paleogeography of the Central Benue Trough. In: Ofoegbo, C. O. (Ed), *The Benue Trough Structure and Evolution*. International Monograph Series Braunschweig, pp. 511 – 419.
- Obaje N. G., 2009. *Geology and Mineral Resources of Nigeria*. Springer-Verlag Berlin Heidelberg, ISSN 0930-0317, ISBN 978-3-540-92685-6, DOI 10. 1007/978-3-540-92685-6.
- Obi, G. C., 2000. Depositional Model for the Campanian-Maastrichtian Anambra Basin, Southern Nigeria, University of Nigeria, Nsukka, Nigeria, Ph. D. Thesis.

- Obi, G. C., Okogbue, C. O., Nwajide, C. S., 2001. Evolution of the Enugu Cuesta: A Tectonically Driven Erosional Process. *Global Journal of Pure Applied Sciences* Vol. 7, pp. 321–330
- Odomoso, S. E., Oloto, I. N. and Omoboriowo, A. O., 2013. Sedimentology and Depositional Environment of the Mid-Maastrichtian Ajali Sandstone, Anambra Basin, Southern Nigeria. *International Journal of Science and Technology*, pp. 3.
- Ojo, O. J. and Akande, S. O., 2003. Facies relationships and Depositional Environments of the Upper Cretaceous Lokoja Formation in the Bida Basin, Nigeria. *Journal of Mining and Geology*, Vol. 39(1), pp. 255- 241
- Olade, M. A. 1975. Evolution of Nigeria's Benue Trough, a Tectonic Model: *Geological Magazine*, Vol.112, pp.575-583.
- Onu, F. K., 2017. The Southern Benue Trough and Anambra Basin Southeastern Nigeria: A Stratigraphic Review. *Journal of Geography, Environment and Earth Science International*, Vol. 12(2), pp. 1-16; Article no. JGEESI.30416, ISSN: 2454-7352.
- Peters, K. E. and Cassa, M. R., 1994. Applied Source Rock Geochemistry. In: *The Petroleum System, From Source to Trap* (L.B. Magoon and W.G. Dow, eds.), AAPG Memoir, 60, Tulsa, OK, pp. 93-117.
- Readings, H. G., 1981. *Sedimentary Environments and Facies*. Blackwell Science Publications, pp. 569.
- Reyment, R. A. and Mörner, N. A., 1977. Cretaceous Transgressions and Regressions Exemplified by the South Atlantic. *Paleontological Society of Japan, Special Paper 1*, pp. 247-261. Shell British Petroleum Development Company of Nigeria Limited publication.
- Reyment, R. A., 1964. Review of Nigerian Cretaceous-Cenozoic Stratigraphy. *Journal of Nigerian Mining, Geology and Metallurgical Society*, Vol. 1, pp. 61-80.
- Reyment, R. A., 1965. In: *Aspects of the Geology of Nigeria*. University of Ibadan Press, Nigeria, pp. 145.
- Rust, B. R. and Jones, B. G., 1987. , The Hawkesbury Sandstone South of Sydney, Australia: Triassic Analogue for the Deposit of Large, Braided River, *Journal of Sedimentary Petrology*, Vol. 57, pp. 316 – 344.

- Salufu, S. O. and Ogunkunle, T. F., 2015. Source Rock Assessment and Hydrocarbon Prospects of Anambra Basin: Salient Indications for Maturity. *The Pacific Journal of Science and Technology*, Vol. 16(1), pp. 336-344
- Tissot, B. P. and Welte, D. H., 1984. *Petroleum Formation and Occurrence*. 2nd ed., Berlin, Springer Verlag, pp. 699.
- Uzoegbu, M. U., Uchebo, U. A. and Okafor, I., 2013a. Lithostratigraphy of the Maastrichtian Nsukka Formation in the Anambra Basin, Southeastern Nigeria. *International Organization of Scientific Research (IOSR); Journal of Environmental Science, Toxi. Food Techno.*, Vol. 5(5), pp. 96-102.
- Uzuakpunwa A. D. B., 1974. The Abakaliki Pyroclastics, Eastern Nigeria. *New Age and Tectonic Implications. Geological Magazine*, Vol. 11, pp. 65 – 70.

## APPENDIX

Appendix I: Granulometric parameters adopted for the grain size analysis of the sandstone samples.

<b>Granulometric parameters</b>		
<b>Statistical measures</b>	<b>Formula</b>	<b>Author</b>
<b>Graphic mean</b>	$\frac{\Phi_{16} + \Phi_{50} + \Phi_{84}}{3}$	Folk and Ward, 1957
<b>Graphic standard deviation (Sorting)</b>	$\frac{(\Phi_{84} - \Phi_{16}) + (\Phi_{95} - \Phi_5)}{4 \quad 6.6}$	Folk and Ward, 1957
<b>Graphic skewness</b>	$\frac{(\Phi_{16} + \Phi_{84} - 2\Phi_{50}) + (\Phi_5 + \Phi_{95} - 2\Phi_{50})}{2(\Phi_{84} - \Phi_{16}) \quad 2(\Phi_{95} - \Phi_5)}$	Folk and Ward, 1957
<b>Graphic kurtosis</b>	$\frac{\Phi_{95} - \Phi_5}{2.44(\Phi_{75} - \Phi_{25})}$	Folk and Ward, 1957

Appendix II: Grain size parameters interpretation (Folk1957)

<b>Mean</b>		<b>Sorting</b>		<b>Skewness</b>		<b>Kurtosis</b>	
<b>Range</b>	<b>Translate</b>	<b>Range</b>	<b>Translate</b>	<b>Range</b>	<b>Translate</b>	<b>Range</b>	<b>Translate</b>
-1.00-0.00	Very coarse sand	<0.35	Very well sorted	>0.30	Strongly fine skewed	<0.67	Very platykurtic
0.00-1.00	Coarse sand	0.35-0.50	Well sorted	0.30-0.10	Fine skewed	0.67-0.9	Platykurtic
1.00-2.00	Medium sand	0.50-0.71	Moderately well sorted	0.10- -0.10	Near symmetrical	0.9-1.11	Mesokurtic
2.00-3.00	Fine sand	0.71-1.0	Moderately sorted	-0.30- -0.10	Coarse skewed	1.11-1.50	Leptokurtic
3.00-4.00	Very fine sand	1.0-2.0	Poorly sorted	>-0.30	Strongly coarse skewed	1.50-3.00	Very leptokurtic
>4.00	Silt	>2.0	Very poorly sorted			>3.00	Extremely leptokurtic